Numerical Flow Model For an Atlantic Coast Barrier Island Tidal Inlet

By T.C. Gopalakrishnan and J.L. Machemehl

UNC Sea Grant Publication UNC-SG-78-02

NUMERICAL FLOW MODEL FOR AN ATLANTIC COAST BARRIER ISLAND TIDAL INLET

By

T.C. GOPALAKRISHNAN AND J.L. MACHEMEHL

This study was partially supported by the Center for Marine and Coastal Studies and the Office of Sea Grant, NOAA, U.S. Department of Commerce, under Grant No. 04-6-158-44054, and the North Carolina Department of Administration. The U.S. Government is authorized to produce and distribute reprints for governmental purposes notwithstanding any copyright that may appear hereon.

SEA GRANT PUBLICATION UNC-SG-78-02

CENTER FOR MARINE AND COASTAL STUDIES PUBLICATION 78-1

APRIL 1978

ABSTRACT

A numerical model for computation of flow in inlets with junction is developed. The Galerkin technique is coupled with a finite element analysis in the flow model. The vertically integrated equations of momentum and mass conservation (Leendertse (1967)) are used with appropriate boundary and initial conditions. The junction conditions are introduced by the time rates of change of energy and mass flux at the junction. A "double sweep" approach is used in solving for the dynamics of flow. A parabolic shape function is adopted in the model to satisfy the requirement of linear independence.

The numerical flow model is verified with field data obtained from the U.S. Army Corps of Engineers (1976) for Carolina Beach Inlet, North Carolina. The U.S. Army Corps of Engineers collected tide and current data in the inlet gorge and Atlantic Intracoastal Waterway in November 1974. The tidal fluctuations in the inlet gorge and tidal velocities in the Atlantic Intracoastal Waterway were used as initial and boundary conditions respectively. The tidal velocities in the inlet gorge and tidal fluctuations in the Atlantic Intracoastal Waterway were computed with the numerical simulation flow model and compared with field data. The Galerkin finite element flow model performed well considering the complex nature of flow in a tidal inlet.

ACKNOWLEDGEMENT

The authors wish to express their thanks to Mrs. Paula Howell for editing and typing the manuscript and to Mr. Larry Watson for the drafting of the figures.

TABLE OF CONTENTS

LIST OF TABLES

LIST OF FIGURES

INTRODUCTION

General

Tidal inlets are major features of the Atlantic Coast barrier islands. The inlets exert a major influence on the stability of the coastline and on the dynamics of coastal estuaries. Tidal inlets affect the coastal processes along the shoreline. They control the circulation and flushing in estuarine systems. Inlets affect navigation, recreation and fish migration.

Coastal engineers concerned with the development of new tidal inlets on sandy barrier islands need simulation models to predict the flow dynamics of tidal inlets. Flow models are also needed to assess the impact of natural or man made alterations to the inlet environment.

Objective of Project

The objective of this project was to develop and calibrate a numerical flow model for a typical Atlantic Coast barrier island tidal inlet.

Review of Literature

The finite difference scheme and the characteristic theory have been used in the development of numerical models for unsteady flow in coastal inlets. Shubinsky et al (1965) analyzed tidal flow in the Sacremento-San Joaquin Delta. They discretised the zone with finite elements but used a finite difference scheme for the analysis. Amein (1975) introduced the effects of channel junctions (via the conservation of mass and energy equations) into an implicit finite difference scheme. Hinwood and Wallis (1975) have reviewed the use of numerical models in tidal hydraulics.

The use of finite element methods for analyzing flow in tidal inlets is of comparatively recent origin. While using the finite element technique two approaches are possible: (1) the methods based on variational principles and (2) the methods of weighted residuals.

Variational principles do not exist for many fluid flow problems because the situations do not yield a functional which has a stationary value within the time and space domain of interest. An extensive discussion on this topic is given by Finlayson (1972). The methods of weighted residuals are, however, quite general and do not require the existence of a functional. Among the many methods of weighted residuals, the Galerkin technique is particularly advantageous when coupled with the finite element analysis. The weighting functions of the Galerkin technique and the shape functions of the finite element have a direct relationship. Moreover, satisfying the boundary conditions using the nodal values has an added advantage when using the Galerkin technique. The effectiveness of this technique in solving initial value problems has been demonstrated in recent years. Taylor and Davis (1975) have analyzed the two dimensional tidal flow in the Southern North Sea using cubic isoparametric elements. They also indicated how implicit equations can be developed (leading to the use of large time steps) when the finite element in time is coupled with the finite element in space.

NUMERICAL FLOW MODEL

The Governing Equations

Taking the atmospheric pressure to be the datum and omitting the tide generating forces, the coriolis force and the wind force, the one-dimensional momentum equation can be written as:

$$\frac{\partial U}{\partial t} + U \frac{\partial U}{\partial x} + g \frac{\partial \eta}{\partial x} + A_f = 0 \quad . \ . \ . \ . \ . \ . \ . \ . \ . \ . \ . \ . \ . \ . \ . \ . \ 1$$

where U is the one-dimensional velocity, η is the instantaneous water level above a reference datum, g is the acceleration due to gravity, A_f is the friction term and x and t are the independent variables of space and time as shown in Figure 1.

The one-dimensional velocity can be mathematically expressed as:

$$U = \frac{1}{(h+\eta)} \int_{-h}^{\eta} u \, dz \quad . \ . \ . \ . \ . \ . \ . \ . \ . \ . \ . \ . \ . \ . \ . \ . \ . \ . \ . \ 2$$

where u is the point velocity and is a function of z at a given section and h is the depth. While adopting the one-dimensional approach the kinematic equation is written as:

$$\frac{\partial \eta}{\partial t} + \frac{\partial ((h+\eta)\ U)}{\partial x} = 0 \quad . \ . \ . \ . \ . \ . \ . \ . \ . \ . \ . \ . \ . \ . \ . \ . \ . \ 3$$

which assumes unit width in the y-direction. In analyzing inlet flow, variation of the area of flow with respect to x must be taken into account; hence, the equation to be used for unsteady flow is written as:

$$\frac{\partial A}{\partial t} + \frac{\partial (AU)}{\partial x} = 0 \quad . \ 4$$

where A is the area of flow and is a function of x and η.

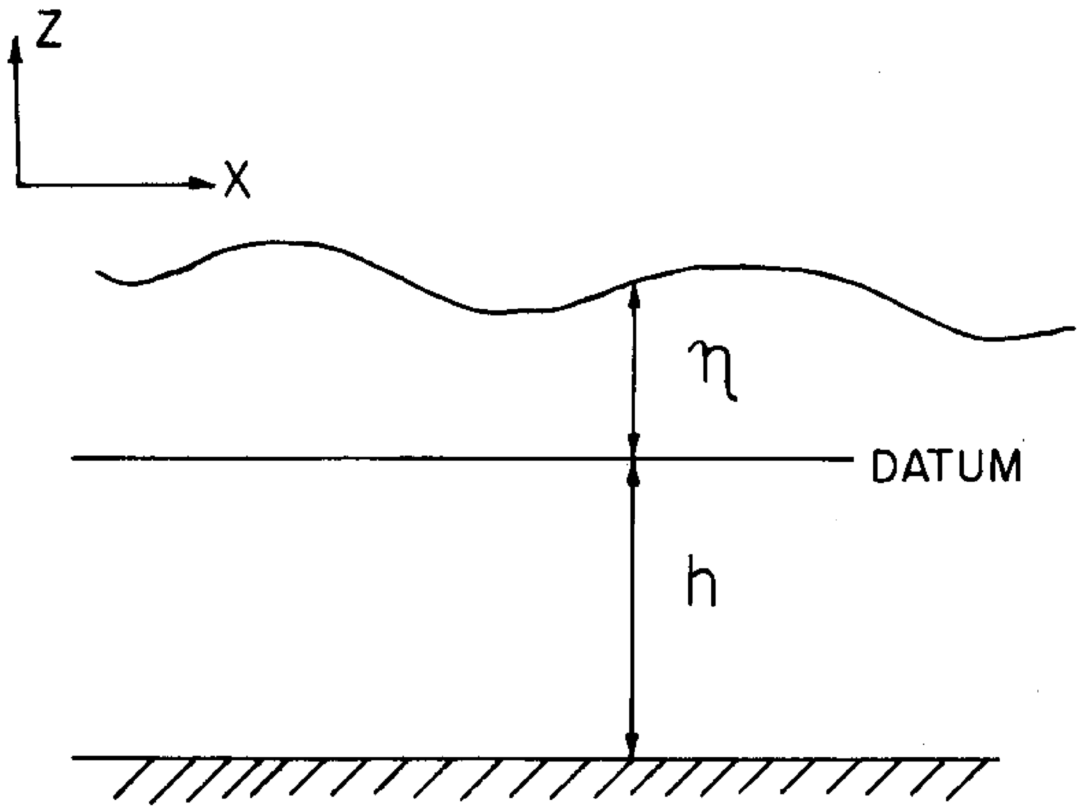

FIGURE 1. DEFINITION SKETCH.

Equations 1 and 4 give the mathematical description of the inlet flow. The friction term in Equation 1 and the area in Equation 4 can be approximated as follows:

(1) The friction term is expressed using Manning's Equation for open channel flow:

$$A_f = gS_f \quad \dots\dots\dots\dots\dots\dots\dots\dots 5$$

The friction slope is given by:

$$S_f = \frac{U^2 n^2}{R^{4/3}} \quad \dots\dots\dots\dots\dots\dots\dots\dots 6$$

where n is Manning's constant, and R is the hydraulic radius.

It should be noted that both the area and wetted perimeter are functions of the instantaneous water level at a given section.

(2) The area of flow can be expressed as a linear function of η following Amein (1975):

$$A = A^0 + A^1\eta \quad \dots\dots\dots\dots\dots\dots\dots\dots 7$$

where A^0 and A^1 are the section parameters.

(3) The wetted perimeter can also be expressed similarly:

$$P = P^0 + P^1\eta \quad \dots\dots\dots\dots\dots\dots\dots\dots 8$$

Equation 4 can now be rewritten as:

$$\frac{\partial(A^0 + A^1\eta)}{\partial t} + \frac{\partial}{\partial x}((A^0 + A^1\eta)U) = 0 \quad \dots\dots\dots\dots 9$$

or

$$A^1 \frac{\partial\eta}{\partial t} + (A^0 + A^1\eta)\frac{\partial U}{\partial x} + U\frac{\partial}{\partial x}(A^0 + A^1\eta) = 0 \quad \dots\dots 10$$

The branches of an inlet are assumed to be of uniform cross section and therefore, A^0 and A^1 are constants for a given channel. Equation 10 can then be written as:

$$A^1 \frac{\partial \eta}{\partial t} + (A^0 + A^1 \eta) \frac{\partial U}{\partial x} + U \cdot A^1 \cdot \frac{\partial \eta}{\partial x} = 0 \quad \ldots\ldots\ldots\ldots \quad 11$$

or

$$\frac{\partial \eta}{\partial t} + (\frac{A^0}{A^1} + \eta) \frac{\partial U}{\partial x} + U \frac{\partial \eta}{\partial x} = 0 \quad \ldots\ldots\ldots\ldots \quad 12$$

Thus, after introducing the approximations, the mathematical model for analyzing inlet flow is given by Equations 13 and 14 .

$$\frac{\partial U}{\partial t} + U \frac{\partial U}{\partial x} + g \frac{\partial \eta}{\partial x} + g(\frac{U^2 n^2}{R^{4/3}}) = 0 \quad \ldots\ldots\ldots\ldots \quad 13$$

$$\frac{\partial \eta}{\partial t} + (\frac{A^0}{A^1} + \eta) \frac{\partial U}{\partial x} + U \frac{\partial \eta}{\partial x} = 0 \quad \ldots\ldots\ldots\ldots \quad 14$$

Junction Conditions. The equations to be satisfied at the junctions of channels are the conservation of mass and energy.

Considering the flow in the channel branches of Figure 2, the following equations can be written:

$$A_1 \cdot U_1 + A_2 \cdot U_2 = A_3 \cdot U_3 \quad \ldots\ldots\ldots\ldots \quad 15$$

$$\frac{U_1^2}{2g} + \eta_1 = \frac{U_3^2}{2g} + \eta_3 \quad \ldots\ldots\ldots\ldots \quad 16$$

$$\frac{U_2^2}{2g} + \eta_2 = \frac{U_3^2}{2g} + \eta_3 \quad \ldots\ldots\ldots\ldots \quad 17$$

The subscripts stand for the respective channels and the quantities U, η, and A refer to the values near the junction. However, while adopting the Galerkin technique in solving the initial value problem under consideration, the time rates of quantities are involved. It is, therefore, advantageous to

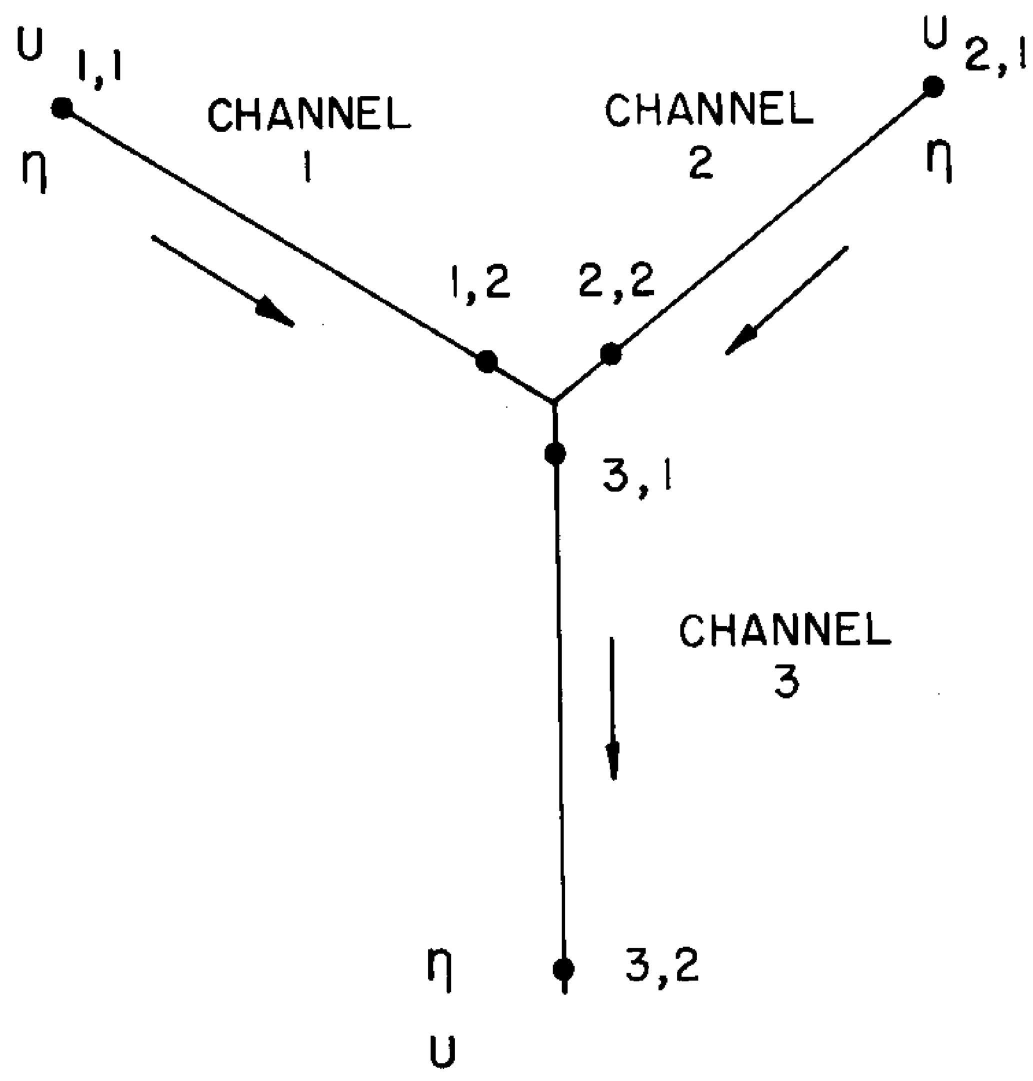

FIGURE 2. FLOW AT JUNCTIONS.

express the junction equations in terms of these rates. Taking the time derivative of quantities in Equations 15, 16 and 17 results in the following equations:

$$(A_1 \frac{\partial U_1}{\partial t} + U_1 \frac{\partial A_1}{\partial t}) + (A_2 \frac{\partial U_2}{\partial t} + U_2 \frac{\partial A_2}{\partial t}) = (A_3 \frac{\partial U_3}{\partial t} + U_3 \frac{\partial A_3}{\partial t}) \quad \ldots \quad 18$$

$$\frac{1}{g} (U_1 \frac{\partial U_1}{\partial t}) + \frac{\partial \eta_1}{\partial t} = \frac{1}{g} (U_3 \frac{\partial U_3}{\partial t}) + \frac{\partial \eta_3}{\partial t} \quad \ldots \quad 19$$

$$\frac{1}{g} (U_2 \frac{\partial U_2}{\partial t}) + \frac{\partial \eta_2}{\partial t} = \frac{1}{g} (U_3 \frac{\partial U_3}{\partial t}) + \frac{\partial \eta_3}{\partial t} \quad \ldots \quad 20$$

Using the dot notation for the time derivatives and remembering that the area of flow is given by Equation 7, the junction Equations 18, 19 and 20 can be simplified to yield the following:

$$A_1 \dot{U}_1 + U_1 A_1^1 \dot{\eta}_1 + A_2 \dot{U}_2 + U_2 A_2^1 \dot{\eta}_2 = A_3 \dot{U}_3 + U_3 A_3^1 \dot{\eta}_3 \quad . \quad 21$$

$$\frac{U_1 \dot{U}_1}{g} + \dot{\eta}_1 = \frac{U_3 \dot{U}_3}{g} + \dot{\eta}_3 \quad \ldots \quad 22$$

$$\frac{U_2 \dot{U}_2}{g} + \dot{\eta}_2 = \frac{U_3 \dot{U}_3}{g} + \dot{\eta}_3 \quad \ldots \quad 23$$

It is to be noted that in Equation 21 the prime used with A denotes the section parameter as defined in Equation 7. The three Equations 21, 22 and 23 contain the six unknowns:

$\dot{U}_1$, $\dot{U}_2$, $\dot{U}_3$, $\dot{\eta}_1$, $\dot{\eta}_2$ and $\dot{\eta}_3$

Three of the unknowns will be supplied from appropriate boundary conditions at the ends of the channels. Solutions are obtained for the remaining three unknowns from the Equations 21, 22 and 23.

<u>Boundary and Initial Conditions</u>. The tidal fluctuations η at the inlet gorge will be supplied as the forcing function. The velocity fluctuations of the downstream ends of the channels

will be given as additional boundary conditions. The initial conditions include the values of velocities and water levels at selected points which serve as the nodes in the numerical scheme. Thus, the boundary and initial conditions for a system of channels shown in Figure 2 will be as follows: (the second subscript stands for the nodes).

$\dot{\eta}_{3,2}$ for all t

$\dot{U}_{1,1}$ for all t

$\dot{U}_{2,1}$ for all t

$\eta_{1,1}, \eta_{1,2}, \eta_{2,1}, \eta_{2,2}, \eta_{3,1}, \eta_{3,2}$ at $t = 0$

$U_{1,1}, U_{1,2}, U_{2,1}, U_{2,2}, U_{3,1}, U_{3,2}$ at $t = 0$

The Galerkin Principle. There are several methods of weighted residuals like the Galerkin, collocation, least squares, etc. In all these methods an approximation function is selected to represent the variables which on substitution in the governing equation yields a residual. This residual is then forced to be zero by adopting a weighting function and making the integral of the product go to zero as shown:

$$\int_D RW = 0 \quad \ldots \quad 24$$

where R stands for the residual, W the weighting function and D the domain under consideration. The different ways of selecting the weighting function leads to different methods of weighted residuals.

The Galerkin technique employs the principle, that, if the solution of the equation (L is an operator, Ø the unknown and f a known function):

$$L\emptyset - f = 0 \quad \ldots \quad 25$$

can be expressed as a combination of functions N_1, N_2, etc.

in an interval I, then the function $L\phi - f$ is orthogonal to each one of those functions in that interval

$$\left.\begin{array}{l} \int_I (L\phi - f)\, N_1 = 0 \\ \int_I (L\phi - f)\, N_2 = 0, \text{ etc.} \end{array}\right\} \qquad 26$$

Assuming an approximation for ϕ in the form:

$$\bar{\phi} = \sum_{i=1}^{m} a_i\, \phi_i \qquad 27$$

where the ϕ_i's are known functions and the a_i's are the unknowns.

Substituting for ϕ in Equation 25 yields:

$$L\bar{\phi} - f = R \qquad 28$$

where R is the residual resulting from the approximation. Imposing the orthogonality condition given by Equation 26 yields:

$$\left.\begin{array}{l} \int_I (L\bar{\phi} - f)\, \phi_1 = 0 \\ \int_I (L\bar{\phi} - f)\, \phi_2 = 0, \text{ etc.} \end{array}\right\} \qquad 29$$

This means that there are m equations to solve for the coefficients a_i, where $i = 1, \ldots, m$.

By comparing Equation 29 with Equation 24 it is seen that the weighting functions in the case of the Galerkin technique are the trial functions chosen to represent the variable as in Equation 27.

Finite Element Method

The inlet system is discretised using line elements, each channel being represented by a single element. The variables inside the element are approximated using the nodal values of the variables and the shape functions:

$$U = \sum_{i=1}^{m} U_i N_i \qquad 30$$

$$\eta = \sum_{i=1}^{m} \eta_i N_i \qquad 31$$

Where U_i and η_i are the nodal values and N_i is the shape function corresponding to that node. Symbol m stands for the number of nodes in an element. In general the shape functions for U and η can be different. In the present analysis the same shape functions are adopted for both the variables for simplicity.

Solution System. On substituting the values of U and η from Equations 30 and 31 into Equations 13 and 19 the following results:

$$\frac{\partial}{\partial t}\left(\sum_{i=1}^{m} U_i N_i\right) + \left(\sum_{i=1}^{m} U_i N_i\right)\frac{\partial}{\partial x}\left(\sum_{i=1}^{m} U_i N_i\right) + g\frac{\partial}{\partial x}\left(\sum_{i=1}^{m} \eta_i N_i\right) + g\left(\sum_{i=1}^{m} S_{f_i} N_i\right) = 0 \qquad 32$$

$$\frac{\partial}{\partial t}\left(\sum_{i=1}^{m} \eta_i N_i\right) + \left(\frac{A^0}{A_1} + \sum_{i=1}^{m} \eta_i N_i\right)\frac{\partial U}{\partial x} + \left(\sum_{i=1}^{m} U_i N_i\right)\frac{\partial}{\partial x}\left(\sum_{i=1}^{m} \eta_i N_i\right) = 0 \qquad 33$$

Rewritten, Equation 32 becomes:

$$\sum_{i=1}^{m} \left(N_i \frac{\partial}{\partial t} U_i\right) = -\left[\left(\sum_{i=1}^{m} U_i N_i\right)\left(\sum_{i=1}^{m} U_i \frac{\partial}{\partial x} N_i\right) + g\sum_{i=1}^{m}\right.$$

$$\eta_i \frac{\partial N_i}{\partial x} + g \sum_{i=1}^{m} S_{f_i} N_i) \Big] \quad \ldots\ldots\ldots\ldots\ldots\ldots \quad 34$$

Similarly, Equation 33 reduces to

$$\sum_{i=1}^{m} (N_i \frac{\partial \eta_i}{\partial t}) = - \Big[(\frac{A^O}{A^I} + \sum_{i=1}^{m} (\eta_i N_i)) \sum_{i=1}^{m} U_i \frac{\partial N_i}{\partial x} + \sum_{i=1}^{m} U_i$$

$$N_i \sum_{i=1}^{m} (\eta_i \frac{\partial N_i}{\partial x}) \Big] \quad \ldots\ldots\ldots\ldots\ldots\ldots \quad 35$$

At the initial time the nodal values of U and η are known and hence the right side of Equations 34 and 35 are functions of x. Equations 34 and 35 can be written as:

$$\sum_{i=1}^{m} N_i \frac{\partial U_i}{\partial t} = f_1(x) \quad \ldots\ldots\ldots\ldots\ldots\ldots \quad 36$$

$$\sum_{i=1}^{m} N_i \frac{\partial \eta_i}{\partial t} = f_2(x) \quad \ldots\ldots\ldots\ldots\ldots\ldots \quad 37$$

Now the Galerkin technique is used; i.e. the terms in Equations 36 and 37 are multiplied by the shape functions $N_j (j=1,m)$ and integrated over the element.

$$\int_{\ell} (N_j \sum_{i=1}^{m} N_i \frac{\partial U_i}{\partial t}) \, dx = \int_{\ell} (f_1(x) \; N_j) \, dx \quad \ldots\ldots \quad 38$$

$$\int_{\ell} (N_j \sum_{i=1}^{m} \frac{\partial \eta_i}{\partial t}) \, dx = \int_{\ell} (f_2(x) \; N_j) \, dx \quad \ldots\ldots \quad 39$$

As the number of nodes is m, there are m equations of the type in Equation 38 and m equations of the type in Equation 39.

The 2m equations thus obtained can be arranged in the matrix form as shown below:

$$[C]_{mxm} \quad \{\dot{U}\}_{mx1} = \{B_1\}_{mx1} \quad \ldots \quad 40$$

$$[C]_{mxm} \quad \{\dot{\eta}\}_{mx1} = \{B_2\}_{mx1} \quad \ldots \quad 41$$

The members of the matrix C are given by

$$C_{i,j} = \int_{\ell} N_i N_j \, dx \quad \ldots \quad 42$$

The column vectors $\dot{U}$ and $\dot{\eta}$ represent the unknown time rate of change of these variables. The column matrices B_1 and B_2 are the quantities obtained from the RHS of Equations 38 and 39.

The solution of the system of Equations 40 and 41 yields the time derivatives of U and η. Using these values, U and η can be advanced in the time domain by a time stepping procedure.

Time Integrations. Assuming that the values of U and η are known at an instant the Euler Predictor-Corrector procedure can be adopted for integration in the time domain.

$$U^p_{t+\Delta t} = U_t + \dot{U}_t \, (\Delta t) \quad \ldots \quad 43$$

$$U^c_{t+\Delta t} = U_t + (\dot{U}_{t+\Delta t} + \dot{U}_t) \, (\Delta t)/2 \quad \ldots \quad 44$$

The superscript p stands for the predictor and c for the corrector. As it can be seen from Equations 43 and 44 the corrector equation is based on the mean of the rates of change at t and $t+\Delta t$. The value of $\dot{U}_{t+\Delta t}$ is obtained by using the predicted values (i.e., U^p). A similar procedure is adopted for η. To test the improvement in accuracy as a result of using higher order predictor-corrector methods the third order Adams Moulton method was used for time integration. The Euler Predictor-Corrector was found to be adequate.

Double Sweep Process. The double sweep process has been used in the past to solve channel networks. This is found to be useful in the present analysis. Here the channels are first solved for U or η as the case may be and after satisfying the junction conditions they are solved for the other unknown. If a purely explicit method is adopted for the time integration then the double sweep technique resulted in instability. However, the predictor-corrector algorithms effectively removed the anomaly introduced by that technique.

Choice of Shape Functions. The trial function in the Galerkin approximation should be such that they satisfy the following conditions: (1) completeness and (2) linear independence.

The first condition implies that the functions must belong to a set taking sufficient terms of which we can approximate any function in the region under consideration. The second states that the functions are not related to each other by a proportionality constant.

An attempt was made to analyze an inlet using the linear and quadratic shape functions commonly used in the finite element method. The linear and quadratic shape functions introduced spurious water slopes which led to oscillatory instability during computation. A parabolic shape function was utilized since the water surface conforms more or less to a parabola. The parabolic shape function for the instantaneous water level was chosen as shown in Figure 3. The same shape function was adopted for the velocity. The parameter 'D' in the expression for the shape function was found characteristic to a particular inlet. This shape function gave good results while at the same time making the convergence rapid.

Conceptual Flow Chart and Computer Program

The conceptual flow chart for the main program is shown in Figure 16 (Appendix A). The computer program with subroutines is shown in Figure 17 (Appendix B). Variables in the computer program are defined in Table 1 (Appendix C).

APPLICATION OF NUMERICAL SIMULATION MODEL

The coastline of the southeastern United States is primarily composed of sandy barrier islands which are separated from the mainland by elongated lagoons containing expansive marshlands. The marshlands or estuarine areas are characterized by salt marsh and shallows interlaced with small tidal channels. The Atlantic Coast barrier islands are breached by tidal inlets. One of these inlets under investigation by the U.S. Army Corps of Engineers (1976) is Carolina Beach Inlet, North Carolina.

Carolina Beach Inlet

Carolina Beach Inlet is located in the coastal zone of

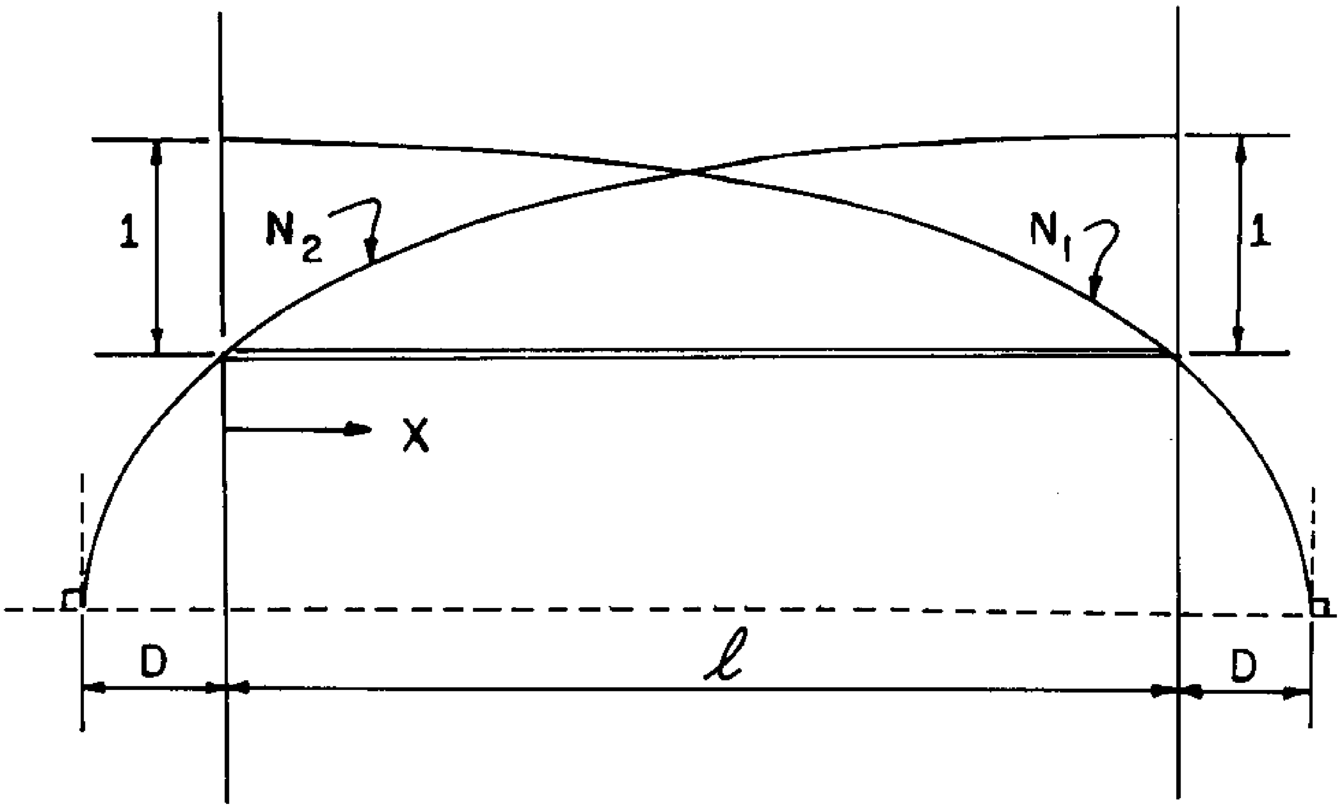

Where:

$$N_1 = \frac{\sqrt{D + \ell - x} - \sqrt{D}}{\quad}$$

$$N_2 = \frac{\sqrt{D + x} - \sqrt{D}}{a}$$

$$a = \sqrt{D + \ell} - \sqrt{D}$$

FIGURE 3. SHAPE FUNCTIONS.

the southeastern region of North Carolina. The Inlet is approximately 18 miles (29 kilometer) north of the Cape Fear River in New Hanover County as shown in Figure 4. A history of the inlets is shown in Figures 5 and 6.

Carolina Beach Inlet was first opened in 1952 by excavating through the barrier island. The inlet connected the 12 ft. (3.7 m) deep Atlantic Intracoastal Waterway (AIWW) through a 15 ft. (4.6 m) deep gorge to the Atlantic Ocean over an ocean bar as shown in Figure 7. The ocean bar was 3 to 4 ft. (0.9 to 1.2 m) deep below mean low water (MLW). The inlet is connected with the Cape Fear River through snows cut as shown in Figure 8. Snows cut was completed in 1970 while connecting channels between the Atlantic Intracoastal Waterway and Masonboro Inlet were completed in 1957.

Hydrographic Cross Sections. The U.S. Army Corps of Engineers (1976) collected hydrographic data for locations shown in Figure 9. Cross sections and cross-sectional areas for ranges 2 through 4 are shown in Figures 10 through 12.

The cross-sectional areas and wetted perimeters were expressed as a linear function of instantaneous water level in the numerical model.

Tide and Current Data. The U.S. Army Corps of Engineers (1976) collected tide and current data at ranges 2 through 4.during November 1974. The tide near range 3 (i.e., $\eta_{3,2}$) in the inlet gorge and the current velocities at range 2 and 3 (i.e., $U_{1,1}$ and $U_{2,1}$) in the Atlantic Intracoastal Waterway were used as initial and boundary conditions respectively.

The inlet was subject to a tidal range of about 4 ft. (1.2 m) an average spring range of 4.7 ft. (1.2 m) and to higher stage resulting from hurricane storm surges.

Model Verification

The model was verified with the tidal and current data supplied by the U.S. Army Corps of Engineers (1976) for Carolina Beach Inlet, North Carolina. The velocities in the inlet gorge (i.e. $U_{3,2}$) and tidal fluctuations in the Atlantic Intracoastal Waterway (i.e. $\eta_{1,1}$ and $\eta_{2,1}$) were computed in the numerical simulation flow model. The computed values for tide and current are given in Appendices D and E and are compared with the field values in Figures 13 through 15.

CONCLUSION

The analysis suggested by Taylor and Davis (1975) has

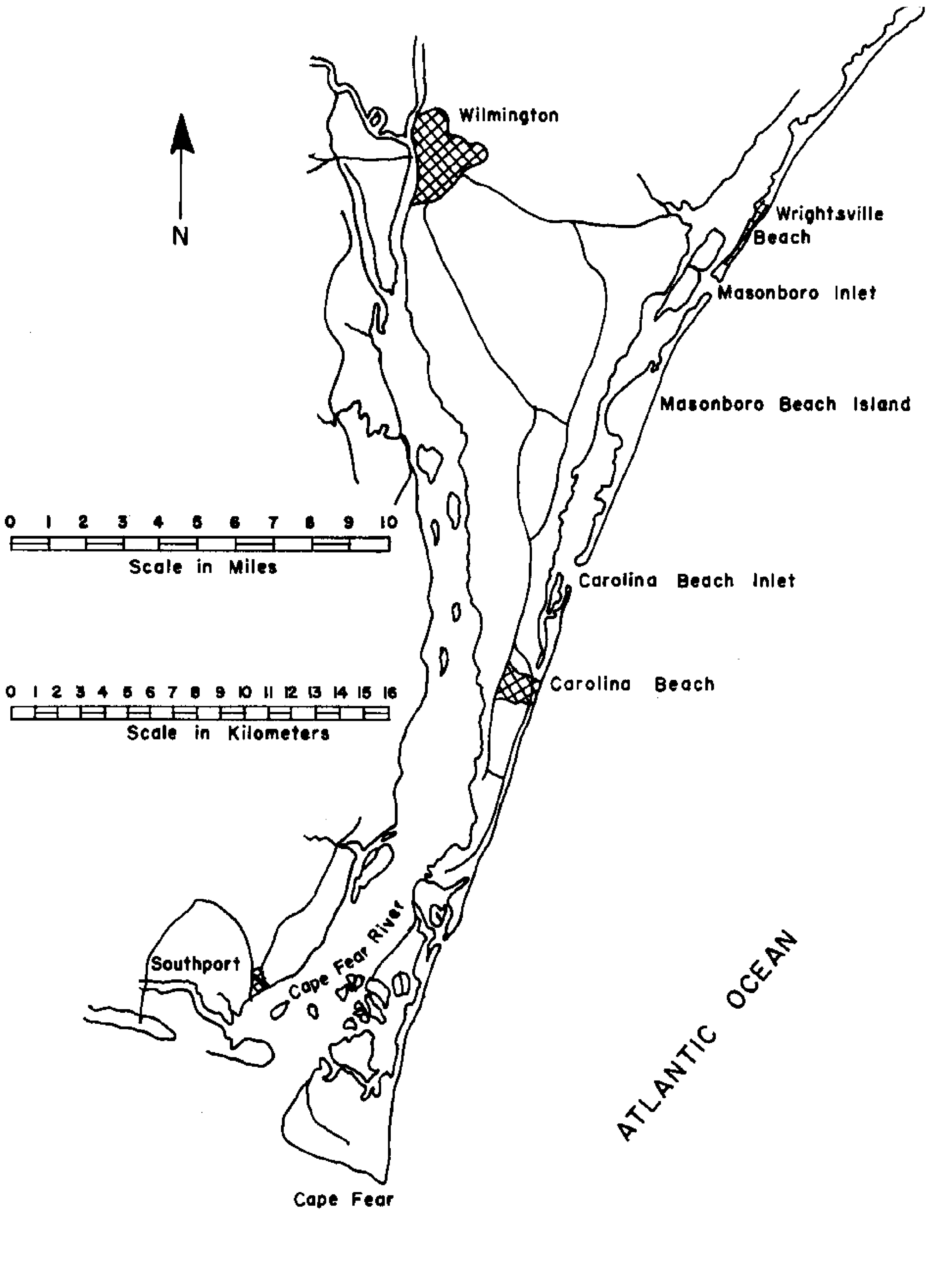

FIGURE 4. LOCATION MAP.

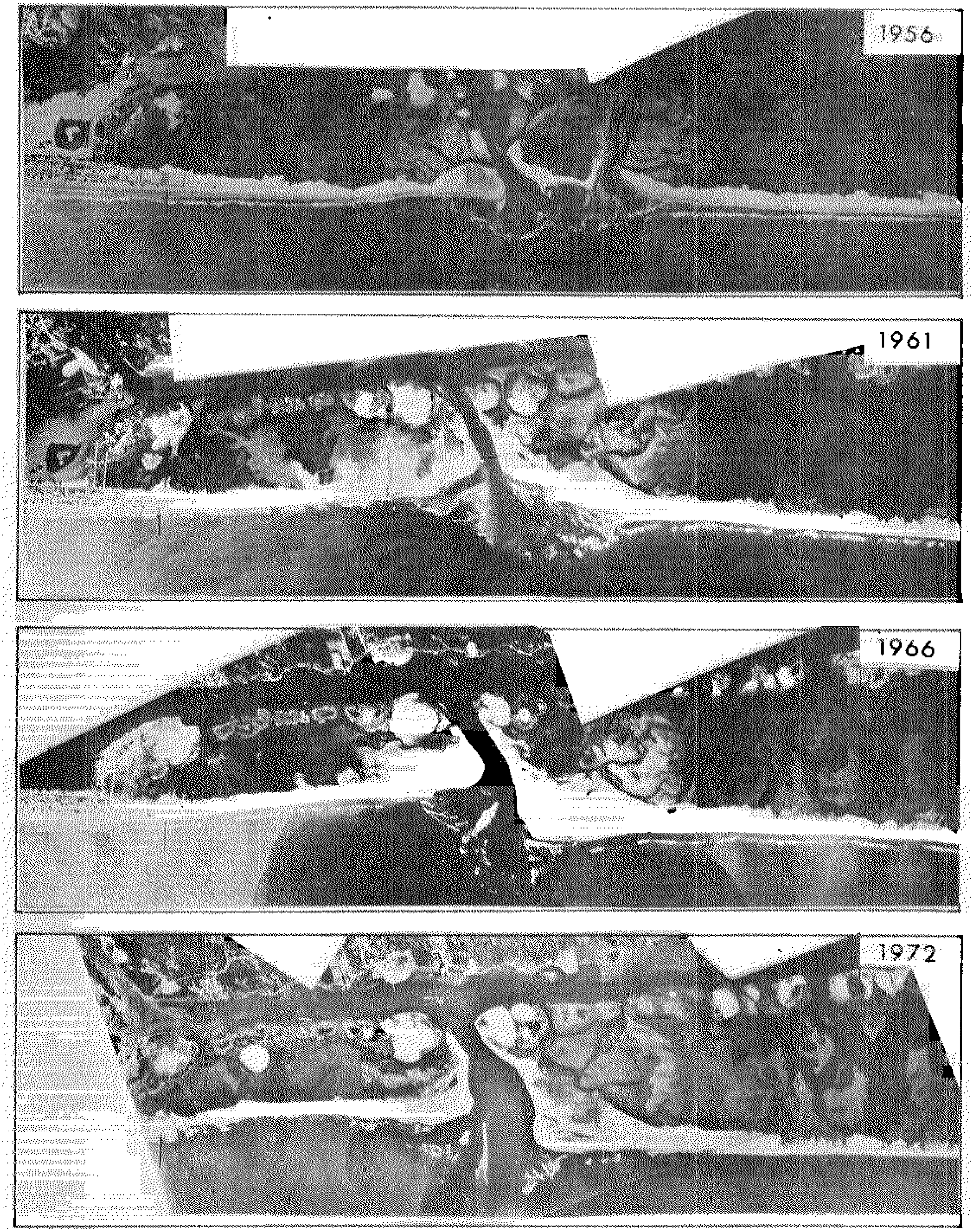

FIGURE 5. CAROLINA BEACH INLET, NORTH CAROLINA FROM 1956 TO 1972.

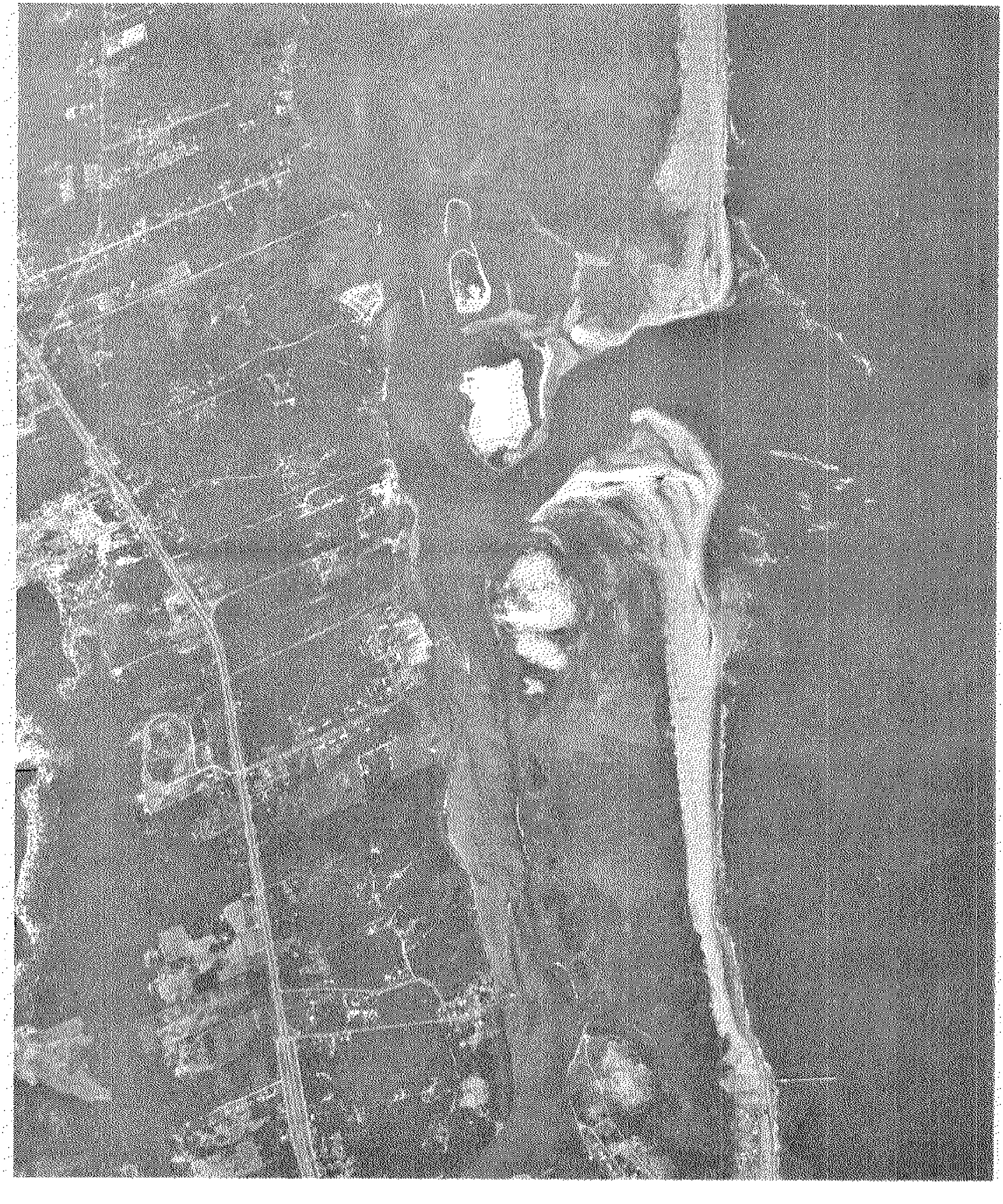

FIGURE 6. CAROLINA BEACH INLET, NORTH CAROLINA IN 1976.

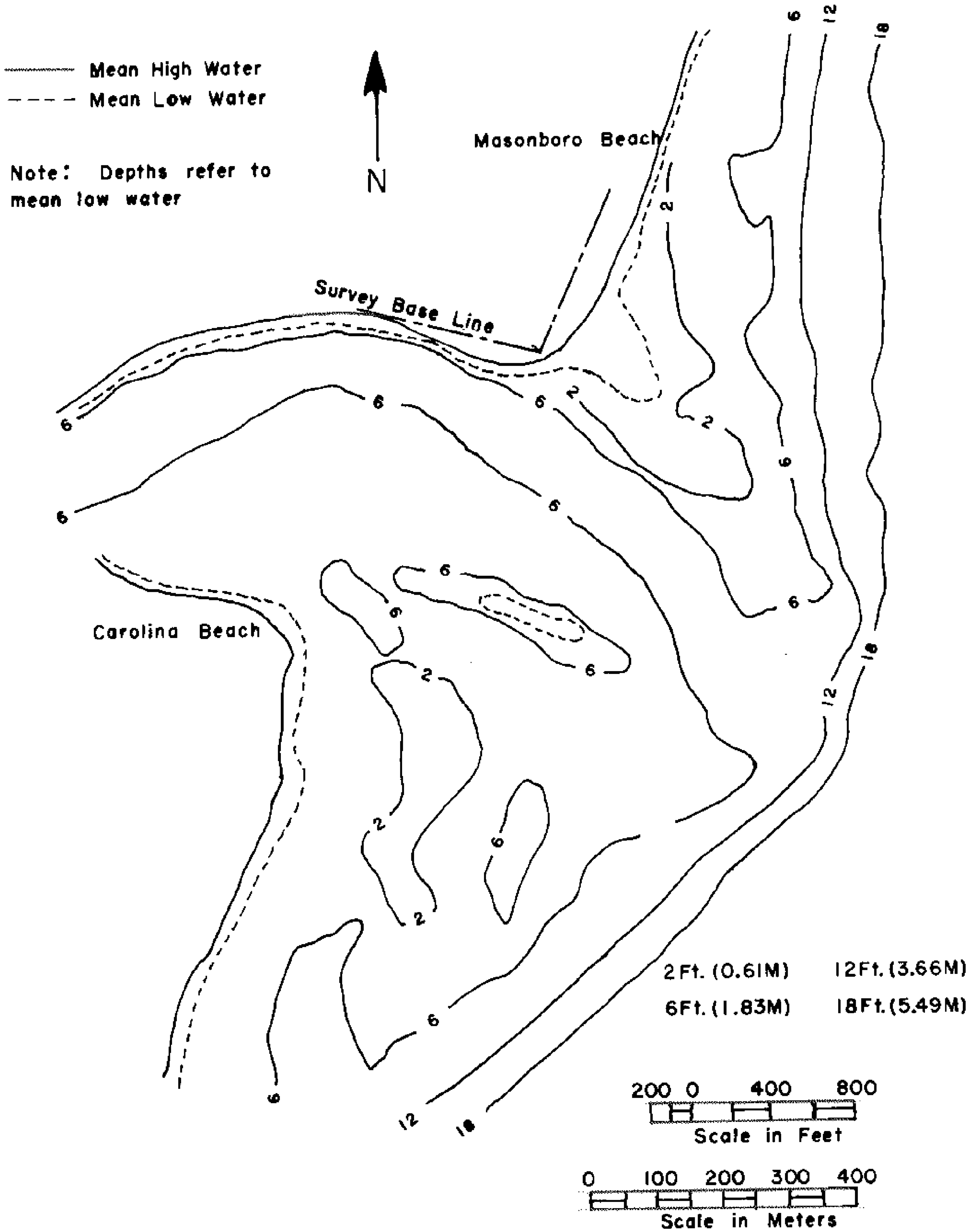

FIGURE 7. CAROLINA BEACH INLET, FEBRUARY 1972.

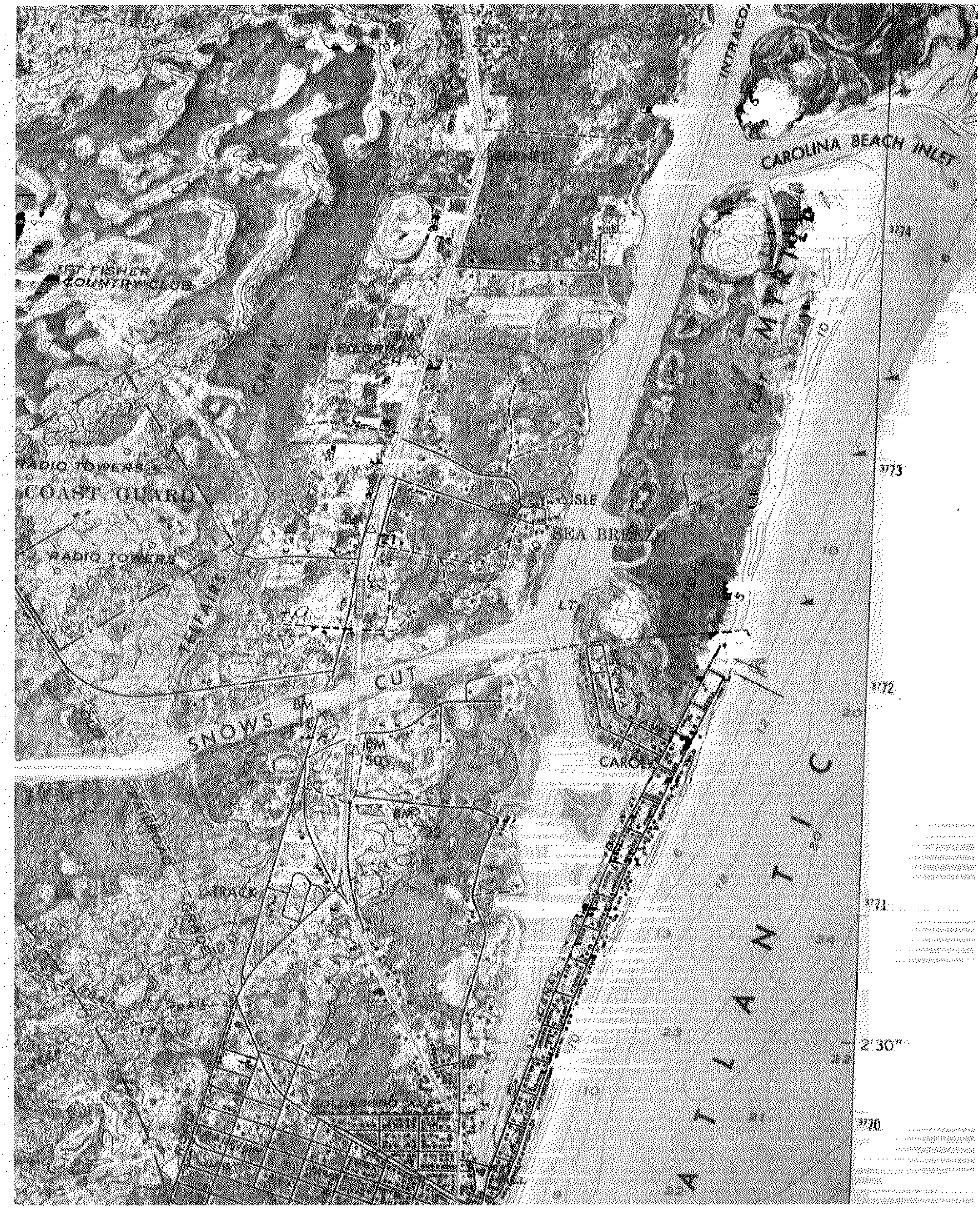

FIGURE 8. ATLANTIC INTRACOASTAL WATERWAY AND SNOWS CUT, NORTH CAROLINA.

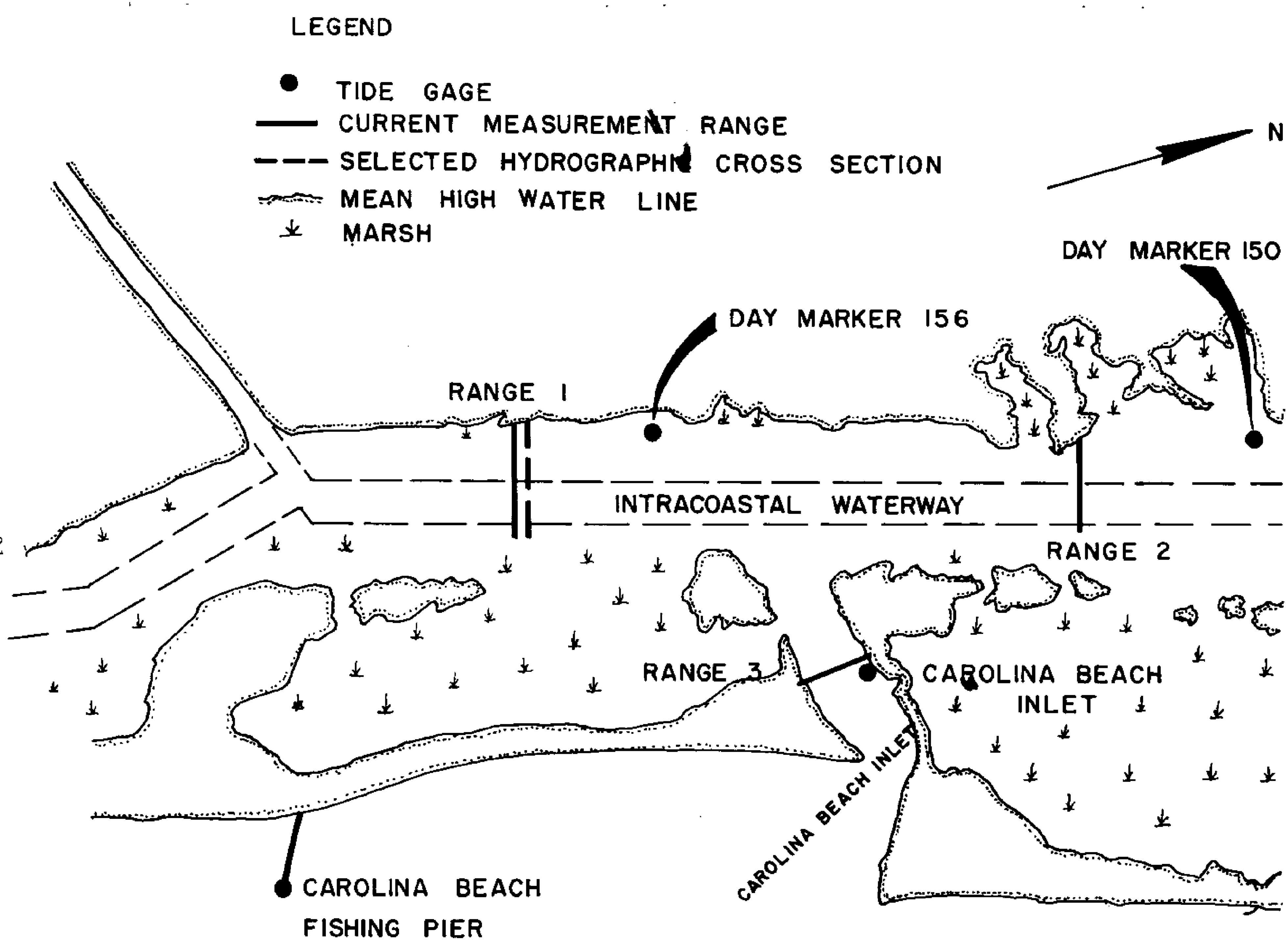

FIGURE 9. CAROLINA BEACH INLET, NORTH CAROLINA.

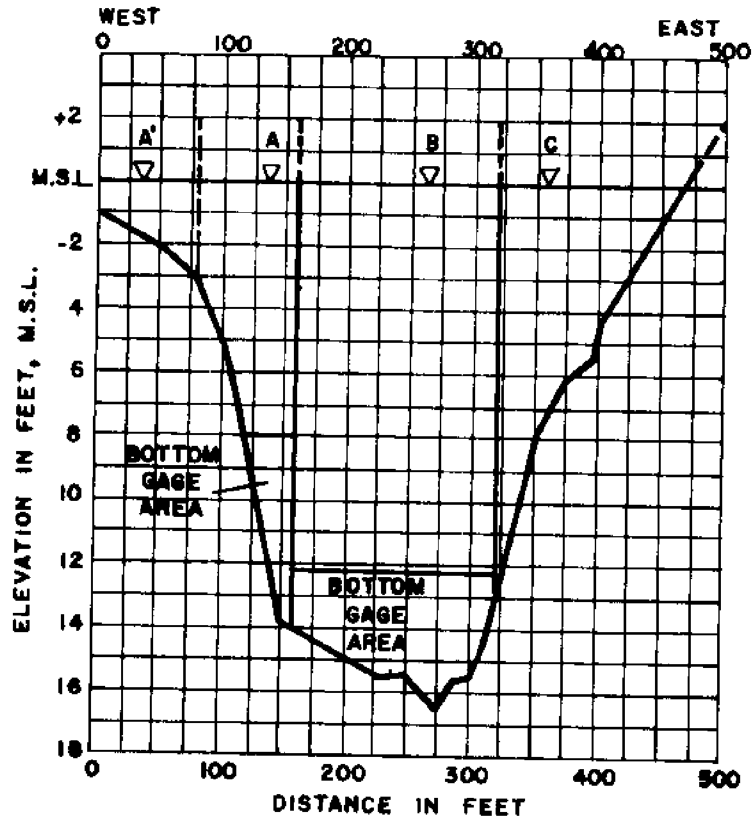

CAROLINA BEACH INLET, RANGE 2

CROSS-SECTIONAL AREAS (ft.²) RANGE 2

STA.	SURFACE GAGE AREA AT			MIDDLE GAGE AREA AT			BOTTOM GAGE AREA AT			TOTAL AREA AT		
	-2	M.S.L.	+2	-2	M.S.L.	+2	-2	M.S.L.	+2	-2	M.S.L.	+2
A'	15	145	290							15	145	290
A	280	320	320	90	210	380	150	150	150	520	680	850
B	650	650	650	640	965	1290	485	485	485	1775	2100	2425
C										520	785	1110
TOTAL AREA OF RANGE										2830	3710	4675

FIGURE 10. HYDROGRAPHIC CROSS-SECTION OF RANGE 2.

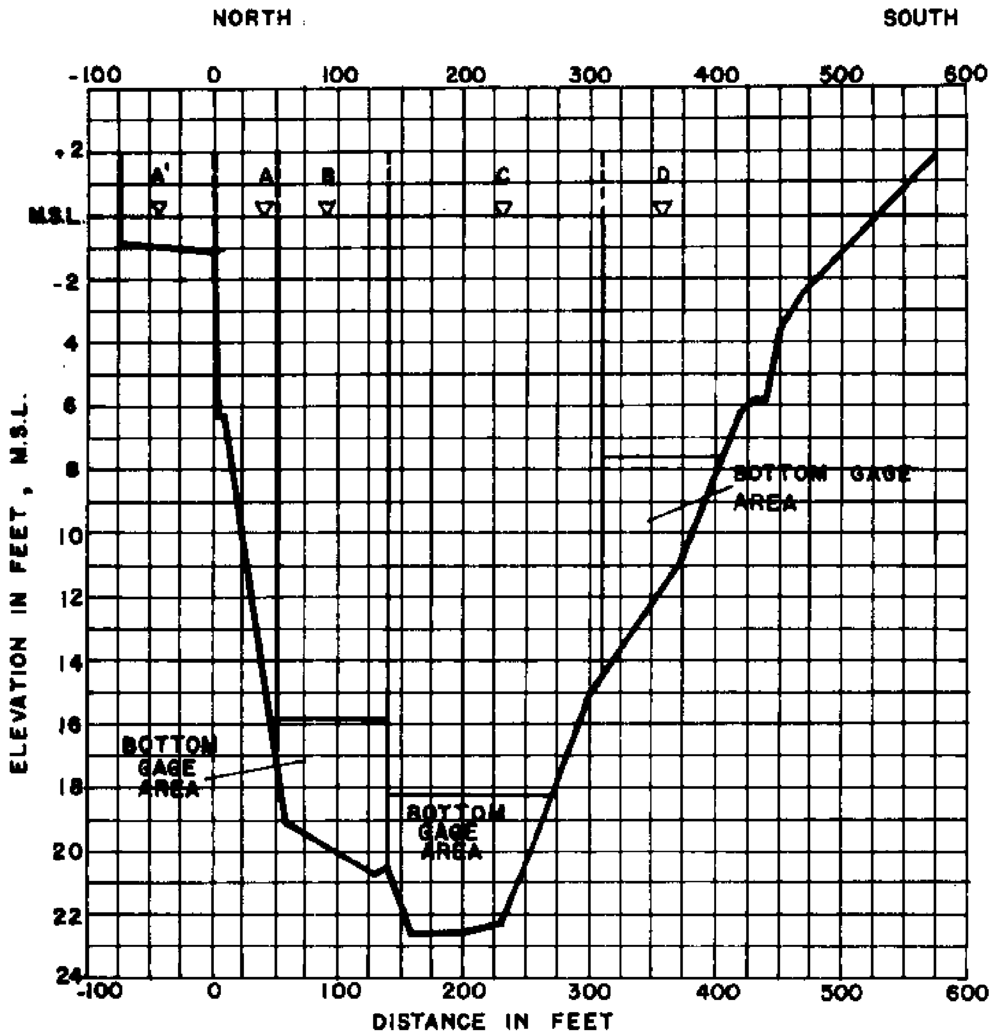

CAROLINA BEACH INLET – RANGE 3

CROSS-SECTION AREAS (ft.²) RANGE 3

STA.	SURFACE GAGE AREA AT			MIDDLE GAGE AREA AT			BOTTOM GAGE AREA AT			TOTAL AREA AT		
	-2	M.S.L.	+2	-2	M.S.L.	+2	-2	M.S.L.	+2	-2	M.S.L.	+2
A'	0	70	210							0	70	210
A	180	185	190	135	225	315	135	135	135	450	545	640
B	360	360	360	880	1060	1240	350	350	350	1590	1770	1950
C	680	680	680	2000	2340	2680	440	440	440	3120	3460	3800
D	560	690	860	180	460	740	310	310	310	1050	1460	1910
TOTAL AREA OF RANGE										6210	7305	8510

FIGURE 11. HYDROGRAPHIC CROSS-SECTION OF RANGE 3.

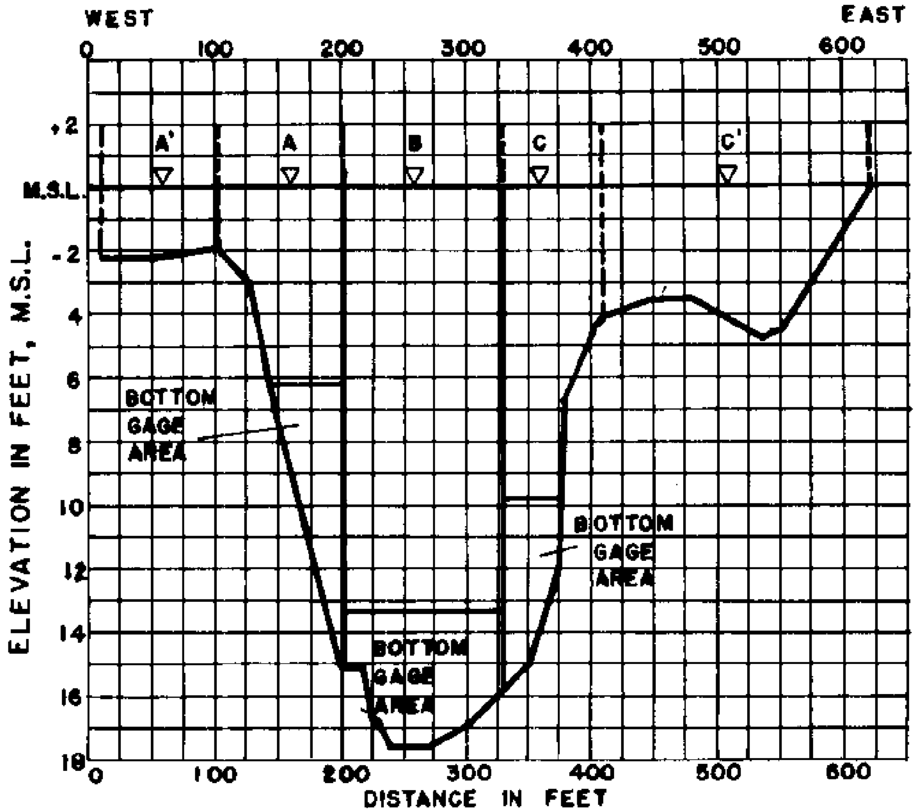

CAROLINA BEACH INLET — RANGE 4

CROSS-SECTIONAL AREAS (ft.^{2}) RANGE 4

STA.	SURFACE GAGE AT			MIDDLE GAGE AT			BOTTOM GAGE AT			TOTAL AREA AT		
	-2	M.S.L.	+2	-2	M.S.L.	+2	-2	M.S.L.	+2	-2	M.S.L.	+2
A'	0	180	360							0	180	360
A										240	520	920
B	525	525	525	940	1205	1465	510	510	510	1975	2240	2500
C	320	320	320	190	320	480	195	195	195	705	835	995
C'	330	720	1012							330	720	1012
TOTAL AREA OF RANGE										3250	4485	5787

FIGURE 12. HYDROGRAPHIC CROSS-SECTION OF RANGE 4.

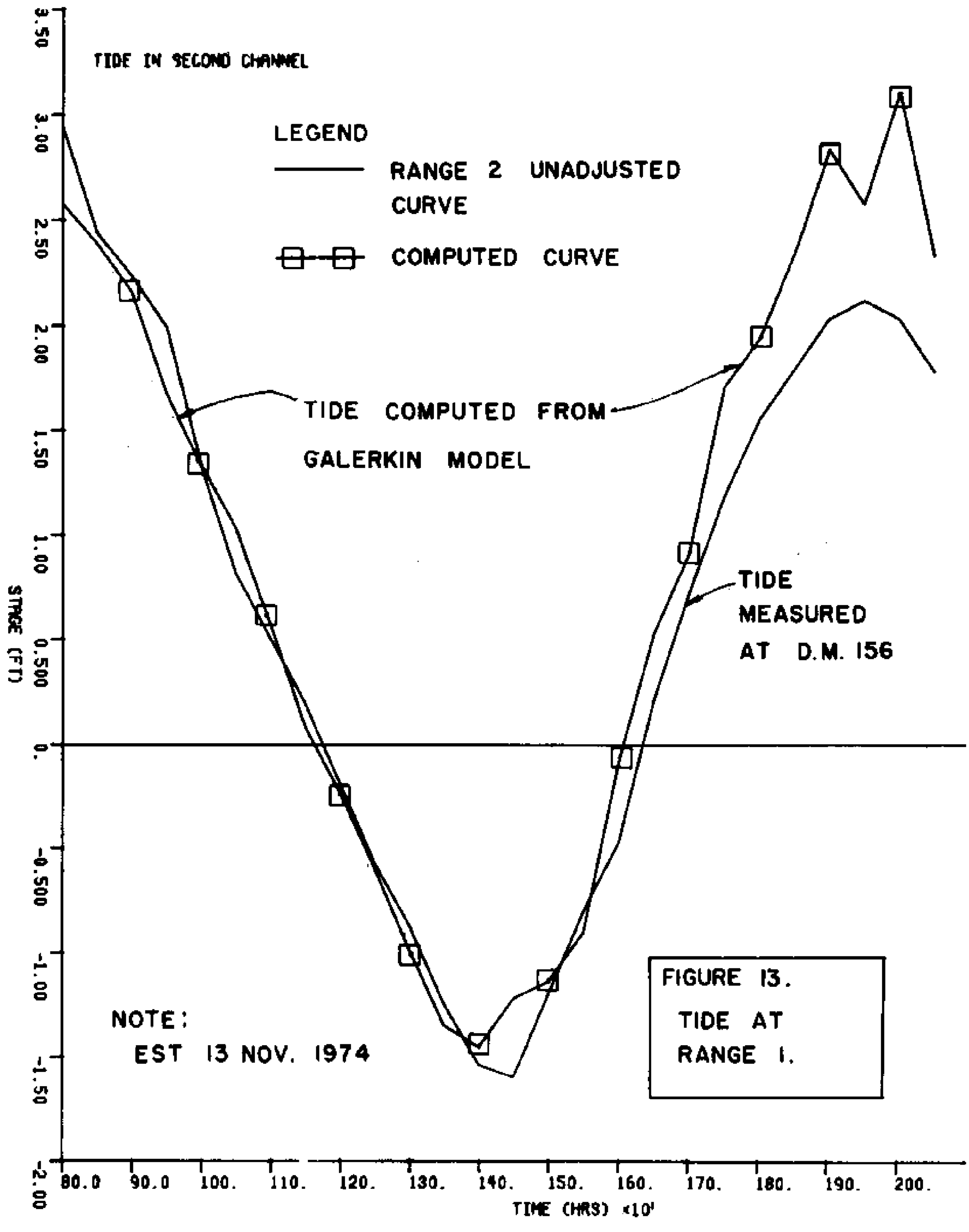

FIGURE 13.
TIDE AT RANGE 1.

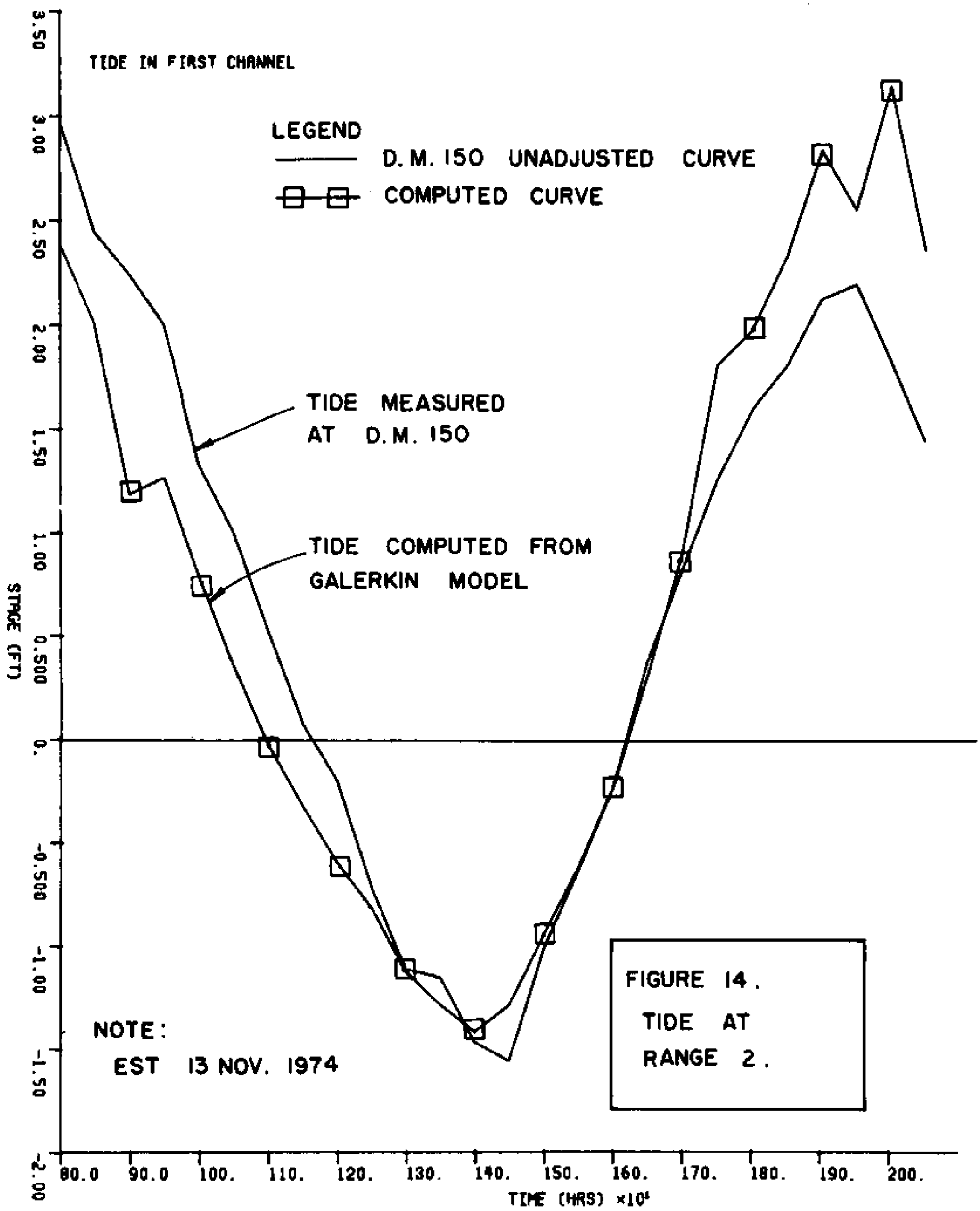
TIDE IN FIRST CHANNEL
LEGEND
D. M. 150 UNADJUSTED CURVE
COMPUTED CURVE
TIDE MEASURED AT D. M. 150
TIDE COMPUTED FROM GALERKIN MODEL
NOTE: EST 13 NOV. 1974
FIGURE 14. TIDE AT RANGE 2.
STAGE (FT)
3.50
3.00
2.50
2.00
1.50
1.00
0.500
0.
-0.500
-1.00
-1.50
-2.00
80.0
90.0
100.
110.
120.
130.
140.
150.
160.
170.
180.
190.
200.
TIME (HRS) ×10¹

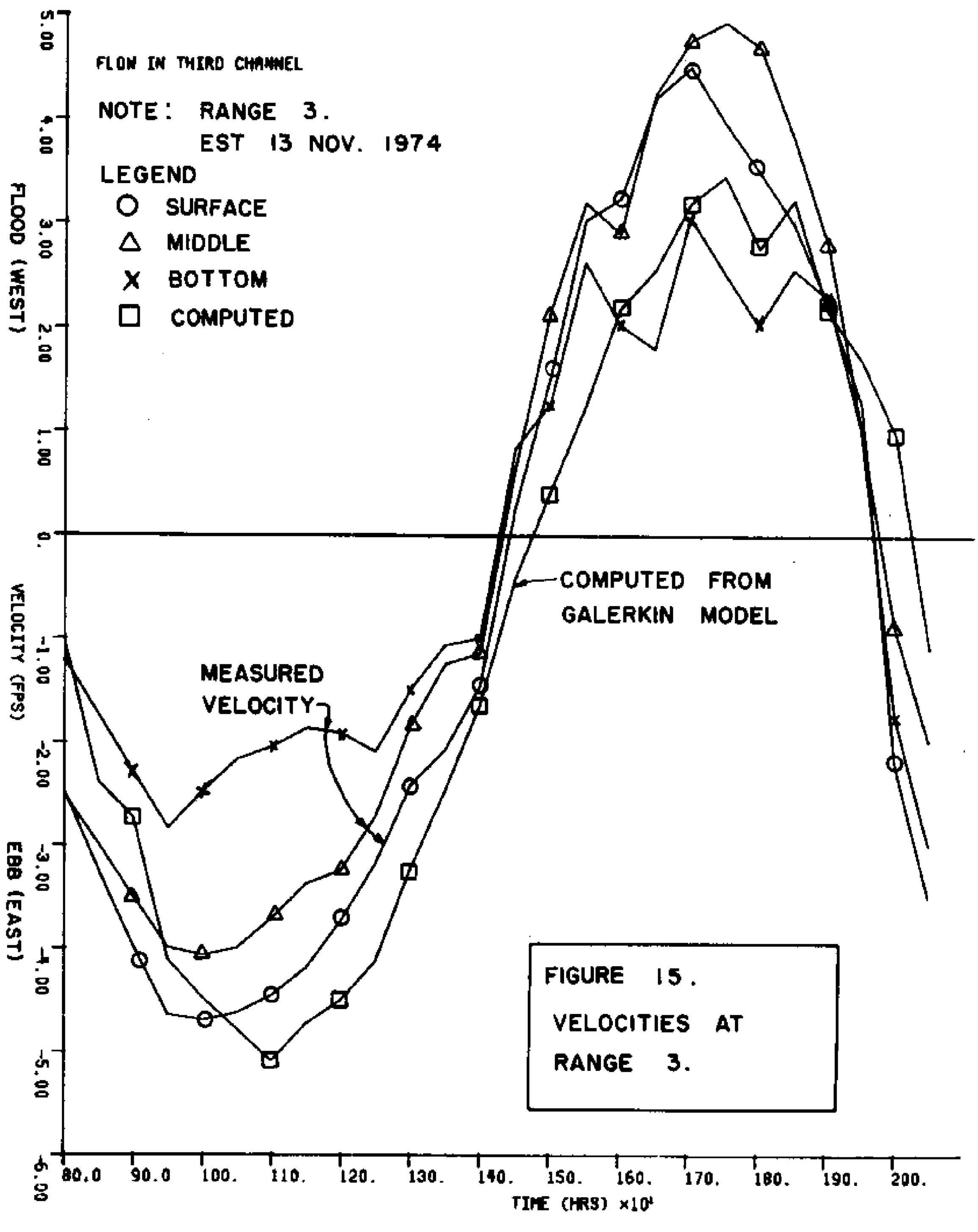

FIGURE 15.
VELOCITIES AT
RANGE 3.

been used for inlets characterised by junctions adopting a one dimensional approach. The vertically integrated equations of momentum and mass conservation (Leendertse (1967)) are used with the appropriate boundary and initial conditions. The Galerkin technique is coupled with the finite element method in analyzing an inlet with channel junctions. The method has several advantages in that the coefficient matrix in the solution system does not change as the model is stepped ahead in time.

The shape function adopted here is problem oriented and is not a general 'basis function.' The parameter 'D' was found to be 700 times the length of the element, ℓ, for Carolina Beach Inlet. The parabolic shape function satisfies only the requirement of linear independence. The completeness requirement was not fulfilled by the shape function; therefore, only long elements of the order of 600 ft. (183 m) to 1000 ft. (305 m) were adopted. For these lengths the error introduced was found to be low.

The Galerkin finite element model for flow in an inlet was found satisfactory considering the complex nature of the flow in a tidal inlet.

REFERENCES

Amein, M., (1975), "Computation of Flow Through Masonboro Inlet, N. C.", Journal, Waterways, Harbors and Coastal Engineering Division, ASCE, Vol. 101, No. WW1, Proc. Paper 11124, pp 93-108.

Finlayson, B. A., (1972), The Method of Weighted Residuals and Variational Principles, Academic Press, New York.

Hinwood, J. B. and I. G. Wallis, (1975), "Review of Models of Tidal Waters", Journal, Hydraulics Division, ASCE, Vol. 101, No. HY11, Proc. Paper 11693, pp 1405-1421.

Leendertse, J.J., (1967), A Computational Model for Long Period Water Wave Propogation, RAND Memorandum, RM-5294-PR, Santa Monice, California.

Shubinsky, R. P., J.C. McCarty and M.R. Lindoy, 1965, "Computer Simulation of Esturile Networks", Journal, Hydraulics Division, ASCE, Vol. 91, No. HY5, Proc. Paper 4470, pp 33-49.

Taylor, C. and J. M. Davis, (1975), "Tidal and Long Wave Propogation - A Finite Element Approach", Computers and Fluids, Vol. 3, pp. 125-148.

U.S. Army Corps of Engineers, (1976), "Data Report for Carolina Beach Inlet, N. C.", USACE Report, Wilmington, N.C.

U.S. Army Corps of Engineers, (1976), "Preliminary Assessment of Alternatives for Navigation Improvements at Carolina Beach Inlet, N.C.", USACE Report, Wilmington, N.C. 122 p.

APPENDICES

APPENDIX A

CONCEPTUAL FLOW CHART FOR MAIN PROGRAM

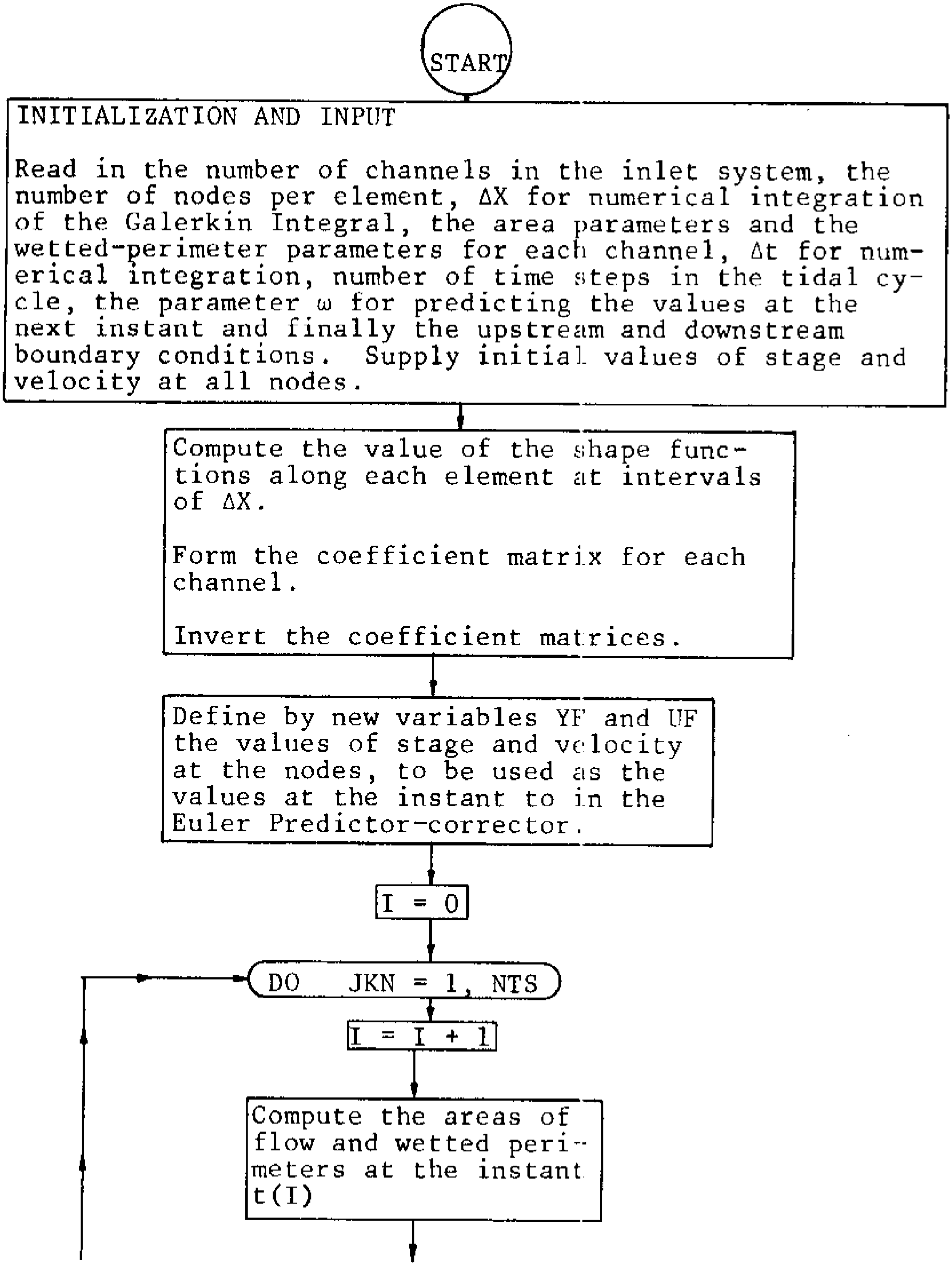

Note: I = Time Instant
NTS = Total Number of Time Steps.

Figure 16. Conceptual Flow Chart for Main Program.

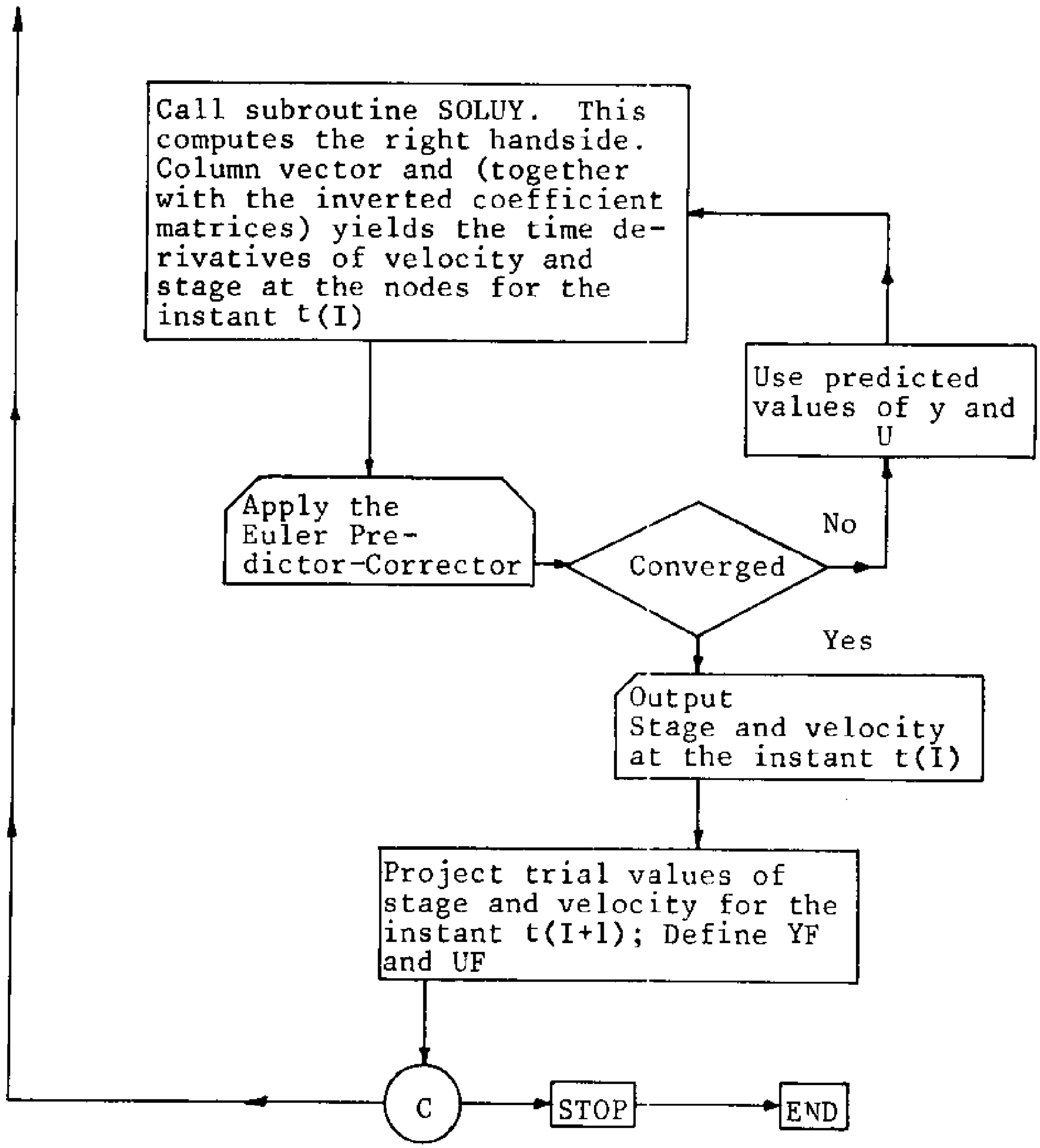

Figure 16. Conceptual Flow Chart for Main Program (Cont.d).

APPENDIX B

COMPUTER PROGRAM

FIGURE 17. COMPUTER PROGRAM.

```
C
C
C                                GALERKIN  ANALYSIS
C                                        OF
C                               CAROLINA  BEACH  INLET
      DIMENSION XB(5),XE(5),MM(5),X(5,11)
      DIMENSION U(5,11),Y(5,11),QD(5,11),YD(5,11),ARO(5),AR1(5),PRO(5),
     1PR1(5),BM(11),C(5,11,11),A01(5),EL(5),Z(10),UF(5,11),YF(5,11),
     2US(5,11),QDF(5,11),YDF(5,11),            AR(5,11),PR(5,11),
     3A(11,11),S(5,11,11),B(11,201),UP(5,11),YP(5,11),P(5)
      DIMENSION QD11(26,3),QD21(26,3),YD33(26,3)
      DIMENSION V1(5),V2(5),AL(5),CK(5),SK(5),C1(5),C2(5),H(5)
      DIMENSION VEL(27)
C
C                   INITIALISATION  AND  INPUT
C
      IQ=3
      FP=700
      P(1)=2 ; P(2)=2 ; P(3)=2
      WRITE (3,10) FP
   10 FORMAT (/T20,'FP =',F7.2)
      READ(1,20) NDEG,NC
   20 FORMAT (5I4)
      N=NDEG+1
      READ (1,30)(EL(J),J=1,NC)
      READ(1,30) DELX
      IDX=DELX
   30 FORMAT (5F8.1)
      READ (1,40) (ARO(J),AR1(J),J=1,NC)
      READ (1,40) (PRO(J),PR1(J),J=1,NC)
   40 FORMAT (8F8.2)
      READ (1,50) DELT
   50 FORMAT (F7.1)
       WRITE (3,60) DELT
   60 FORMAT (//T20,'DELT',F8.2//)
      READ (1,70) W
   70 FORMAT (14F5.2)
      READ (1,70) ((YD33(I,J),J=1,3),I=1,26)
      READ(1,70) ((QD11(I,J),J=1,3),I=1,26)
      READ(1,70) ((QD21(I,J),J=1,3),I=1,26)
      G=9.81 ; AN=0.005
      DO 80 J=1,NC ; DO 80 I=1,N
      U(J,I)=0.0001
   80 Y(J,I)=4.14/3.28
      DO 90 J=1,NC
      IXE=EL(J) ; MM(J)=IXE/IDX
      XB(J)=FP*EL(J)
      H(J)= ((XB(J)+EL(J))**(1/P(J))-XB(J)**(1/P(J))) **P(J)
      ARO(J)=ARO(J)/10.7584
      AR1(J)=AR1(J)/3.28
      A01(J)=ARO(J)/AR1(J)
   90 PRO(J)=PRO(J)/3.28
```

FIGURE 17. COMPUTER PROGRAM (CON'T.)

```
      C
      C                    SHAPE   FUNCTIONS  AND
      C
      C                      COEFFICIENT  MATRIX
      C
            DO 140 J=1,NC ; M=MM(J) ; MP1=M +1 ; MM1=M-1
            DO 100 I=1,MP1
            DA=((EL(J)+XB(J)-DELX*(I-1))/H(J))**(1/P(J))  -(XB(J)/H(J))**(1/P(J
           1))
            DB=((XB(J)+DELX*(I-1))/H(J))**(1/P(J))    -(XB(J)/H(J))**(1/P(J))
            B(1,I)=DA*DA
            B(2,I)=DA*DB
        100 B(3,I)=DB*DB
            DO 130 L=1,3 ; A(L,1)=0
            DO 110 K=2,M,2
        110 A(L,1)=B(L,K)*4+A(L,1)
            DO 120 K=3,MM1,2
        120 A(L,1)=B(L,K)*2+A(L,1)
        130 A(L,1)=(B(L,1)+A(L,1)+B(L,MP1))*DELX/3
            A(2,2)=A(3,1) ; A(1,2)=A(2,1)
            JZ=J
            CALL GINV (A,C,N,JZ,B)
        140 CONTINUE
            DO 150 I=1,NC
            DO 150 J=1,N
            YF(I,J)=Y(I,J)
        150 UF(I,J)=U(I,J)
            NC=IQ
      C
```

FIGURE 17. COMPUTER PROGRAM (CON'T.)

```
C                      SOLUTICN   FOR   THE   DERIVATIVES
C
          ORI=3 ; VP=12 ; DI=-13
          VEL(1)=ORI*SIN(VP*3.1412/DI)
          DO  320 JKN=1,26
          VEL(JKN+1)=ORI*SIN((JKN+VP)*3.1412/DI)
          QD(1,1)=(VEL(JKN+1)-VEL(JKN))/1800/3.28
          QD(2,1)=QD(1,1)*0.8
          DO  310 LLM=1,3
          YD(IQ,N)=YD33(JKN,LLM)/3.28/1800.
          LB=600/DELT
          LD=1 ; LC=LB/LD
          DO  300 LA=1,LC
          DO  290 LLN=1,LD
          NA=0
      160 DO 170 J=1,NC
          DO 170 I=1,N
          AR(J,I)=AR0(J)+AR1(J)*Y(J,I)
      170 PR(J,I)=PR0(J)+PR1(J)*Y(J,I)
          NA=NA+1
          CALL      SOLUY(U,Y,QD,YD,AR,PR,A01,N,S,EL,AN,G,NC,C,UF,YF,DELT,A
         1R1,P,IQ,V1,V2,AL,CK,SK,VV,MM,DELX,XB,H)
```

FIGURE 17. COMPUTER PROGRAM (CON'T.)

```
C
C                        INTEGRATION  BY  THE  EULER  PREDICTOR-CORRECTOR
C
      IF (JKN-1) 180,180,220
  180 IF(LLN-1) 190,190,220
  190 IF (NA-1) 200,200,220
  200 DO 210 I=1,NC ; DO 210 J=1,N
      YDF(I,J)=YD(I,J)
  210 QDF(I,J)=QD(I,J)
  220 DO 230 I=1,NC ; DO 230 J=1,N
      Y(I,J)=YF(I,J)+(YD(I,J)+YDF(I,J))/2.*DELT
  230 U(I,J)=UF(I,J)+(QD(I,J)+QDF(I,J))/2.*DELT
      IF (NA-1) 240,240,260
  240 DO 250 J=1,NC ; DO 250 I=1,N
  250 US(J,I)=U(J,I)
      GO TO 160
  260 DO 270 J=1,NC ; DO 270 I=1,N
      IF ( ABS(US(J,I)/U(J,I)-1.)-0.01) 270,270,240
  270 CONTINUE
C
C                        TRIAL VALUES FOR THE NEXT  STEP
C
      DO 280 I=1,NC ; DO 280 J=1,N
      QDF(I,J)=QD(I,J) ; YDF(I,J)=YD(I,J)
      UP(I,J)=UF(I,J) ; YP(I,J)=YF(I,J)
      UF(I,J)=U(I,J)
      YF(I,J)=Y(I,J)
      U(I,J)=U(I,J)+W*(U(I,J)-UP(I,J))
  280 Y(I,J)=Y(I,J)+(Y(I,J)-YP(I,J))*W
  290 CONTINUE
  300 CONTINUE
  310 CONTINUE
C
C                        OUTPUT
C
      AJKN=JKN
      TIME=AJKN*0.5
      WRITE (3, 330) TIME
      WRITE (3, 340) (Y(I,1),Y(I,N),U(I,1),U(I,N),I=1,NC)
  320 CONTINUE
  330 FORMAT (/T20,'TIME',T30,F6.2)
  340 FORMAT (/T10,2F12.3,5X,2F12.3)
      STOP
      END
```

FIGURE 17. COMPUTER PROGRAM (CON'T.)

```
C                      SUBROUTINE  FOR  INVERSION
C
      SUBROUTINE GINV(A,C,N,JZ,B)
      DIMENSION A(11,11),C(5,11,11),B(11,201)
      DO 1 I=1,N;DO 1 J=1,N
    1 B(I,J)=A(I,J)
      J1=N+1;J2=2*N
      DO 2 I=1,N;DO 2 J=J1,J2
    2 B(I,J)=0.0
      DO 3 I=1,N
      J=I+N
    3 B(I,J)=1.0
      DO 610 K=1,N
      KP1=K+1
      IF (K .EQ. N) GO TO 500
      L=K
      DO 400 I=KP1,N
  400 IF( ABS(B(I,K)) .GT.  ABS(B(L,K))) L=I
      IF (L .EQ. K) GO TO 500
      DO 410 J=K,J2
      TEMP=B(K,J)
      B(K,J)=B(L,J)
  410 B(L,J)=TEMP
  500 DO 501 J=KP1,J2
  501 B(K,J)=B(K,J)/B(K,K)
      IF (K .EQ. 1) GO TO 600
      KM1=K-1
      DO 510 I=1,KM1
      DO 510 J=KP1,J2
  510 B(I,J)=B(I,J)-B(I,K)*B(K,J)
      IF (K .EQ. N) GO TO 700
  600 DO 610 I=KP1,N
      DO 610 J=KP1,J2
  610 B(I,J)=B(I,J)-B(I,K)*B(K,J)
  700 DO 701 I=1,N
      DO 701 J=1,N
      K=J+N
  701 C(JZ,I,J)=B(I,K)
      RETURN
      END
```

FIGURE 17. COMPUTER PROGRAM (CON'T.)

```
      [illegible]
      SUBROUTINE BM1(DELX,VV,MM,BM,J,G,AN,EL,AR,PR,U,Y,XB,H,P)
      DIMENSION EL(5),MM(5),BM(5),B(11,201),AR(5,11),PR(5,11),XB(5),
     1U(5,11),Y(5,11),H(5),P(5)
      R=AR(J,1)/PR(J,1)
      SF1=U(J,1)**2*AN**2/R**(4./3.)
      R=AR(J,2)/PR(J,2)
      SF2=U(J,2)**2*AN**2/R**(4./3.)
      M=MM(J)
      MM1=M-1 ; MP1=M+1 ; BM(1)=0 ; BM(2)=0
      DO 10 I=1,MP1
      DA=((EL(J)+XB(J)-DELX*(I-1))/H(J))**(1/P(J)) -(XB(J)/H(J))**(1/P(J
     1))
      DB=((XB(J)+DELX*(I-1))/H(J))**(1/P(J))    -(XB(J)/H(J))**(1/P(J))
      DAD=(1/P(J)   )*(-1)*((EL(J)+XB(J)-DELX*(I-1))/H(J))**(1/P(J)-1)
      DBD=(1/P(J)   )*((XB(J)+DELX*(I-1))/H(J))**(1/P(J)-1)
      ORD=(U(J,1)*DA+U(J,2)*DB)*(U(J,1)*DAD+U(J,2)*DBD)+
     1G*(Y(J,1)*DAD+Y(J,2)*DBD)+
     2G*(SF1*DA+SF2*DB)
      B(1,I)=ORD*DA
   10 B(2,I)=ORD*CB
      DO 40 L=1,2
      DO 20 K=2,M   ,2
   20 BM(L)=4*B(L,K)+BM(L)
      DO 30 K=3,MM1,2
   30 BM(L)=2*B(L,K)+BM(L)
   40 BM(L)=(   B(L,1)+BM(L)+B(L,MP1))*DELX    /3
      BM(1)=-BM(1) ; BM(2)=-BM(2)
      RETURN ; END
      SUBROUTINE BM2(MM,BM,J,A01,VV,EL,U,Y,DELX,XB,H,P)
      DIMENSION MM(5),BM(5),A01(5),EL(5),B(11,201),U(5,11),Y(5,11),XB(5)
      DIMENSION H(5),P(5)
      M=MM(J)
      MM1=M-1 ; MP1=M+1 ; BM(1)=0 ; BM(2)=0
      DO 10 I=1,MP1
      DA=((EL(J)+XB(J)-DELX*(I-1))/H(J))**(1/P(J)) -(XB(J)/H(J))**(1/P(J
     1))
      DB=((XB(J)+DELX*(I-1))/H(J))**(1/P(J))    -(XB(J)/H(J))**(1/P(J))
      DAD=(1/P(J)   )*(-1)*((EL(J)+XB(J)-DELX*(I-1))/H(J))**(1/P(J)-1)
      DBD=(1/P(J)   )*((XB(J)+DELX*(I-1))/H(J))**(1/P(J)-1)
      ORD=A01(J)*(U(J,1)*DAD+U(J,2)*DBD)+
     1     (Y(J,1)*DA+Y(J,2)*DB)*(U(J,1)*DAD+U(J,2)*DBD)+
     2     (U(J,1)*DA+U(J,2)*DB)*(Y(J,1)*DAD+Y(J,2)*DBD)
      B(1,I)=ORD*CA
   10 B(2,I)=ORD*CB
      DO 40 L=1,2
      DO 20 K=2,M   ,2
   20 BM(L)=4*B(L,K)+BM(L)
      DO 30 K=3,MM1,2
   30 BM(L)=2*B(L,K)+BM(L)
   40 BM(L)=(   B(L,1)+BM(L)+B(L,MP1))*DELX    /3
      BM(1)=-BM(1) ; BM(2)=-BM(2)
      RETURN ; END
```

FIGURE 17. COMPUTER PROGRAM (CON'T.)

```
C                      SUBROUTINE FOR THE TIME DERIVATIVES OF U AND Y
C
      SUBROUTINE SOLUY(U,Y,QD,YD,AR,PR,A01,N,S,EL,AN,G,NC,C,UF,YF,DELT,A
     1R1,P,IQ,V1,V2,AL,CK,SK,VV,MM,DELX,XB,H)
      DIMENSION U(5,11),Y(5,11),QD(5,11),YO(5,11),AR(5,11),PR(5,11),
     1A01(5),S(5,11,11),EL(5),C(5,11,11),UF(5,11),YF(5,11),BM(11),AR1(5)
     2,P(5),X(5,11),MM(5),XB(5),XE(5),H(5),V1(5),V2(5),AL(5),CK(5),SK(5)
      NI=2
      DO 350  J=1,NI
      CALL        BM1(DELX,VV,MM,BM,J,G,AN,EL,AR,PR,U,Y,XB,H,P)
      SUM=0  ; DO 349  I=2,N
  349 SUM=C(J,1,I)*BM(I)+SUM
      BM(1)=(QD(J,1)-SUM)/C(J,1,1)
      DO 350  K=1,N ; QD(J,K)=0
      DO 350  I=1,N
  350 QD(J,K)=QD(J,K)+C(J,K,I)*BM(I)
      J=IQ
      CALL        BM2(MM,BM,J,A01,VV,EL,U,Y,DELX,XB,H,P)
      NM1=N-1
      SUM=0 ; NM1=N-1  ; DO 360  I=1,NM1
  360 SUM=C(J,N,I)*BM(I)+SUM
      BM(N)=(YD(3,N)-SUM)  /C(J,N,N)
      DO 370  K=1,N ; YD(J,K)=0  ; DO 370  I=1,N
  370 YD(J,K)=YD(J,K)+C(J,K,I)*BM(I)
C
      IF (IQ-1) 401,401,374
  374 WAS=0
      N1=N ;  N2=N ;  N3=N
C
```

FIGURE 17. COMPUTER PROGRAM (CON'T.)

```
C
      AX=AR(2,N2)*QD(2,N2)+AR(1,N1)*QD(1,N1)-AR1(3)*YD(3,1)*U(3,1)
      BX=YD(3,1)-QD(1,N1)*U(1,N1)/9.81
      CX=YD(3,1)-QD(2,N2)*U(2,N2)/9.81
      GX=U(3,1)/9.81;AJX=AR(3,1);AKX=AR1(2)*U(2,N2)
      ALX=AR1(1)*U(1,N1)
      QD(3,1)=(AX+AKX*CX+BX*ALX)/(AJX-GX*AKX-GX*ALX)
      YD(1,N1)=BX+QD(3,1)*GX
      YD(2,N2)=CX+QD(3,1)*GX
C
      J=3
      CALL       BM1(DELX,VV,MM,BM,J,G,AN,EL,AR,PR,U,Y,XB,H,P)
      SUM=0  ; DO 380 I=2,N
  380 SUM=C(J,1,I)*BM(I)+SUM
      BM(1)=(QD(J,1)-SUM)/C(J,1,1)
      DO 390 K=1,N ; QD(J,K)=0 ; DO 390 I=1,N
  390 QD(J,K)=QD(J,K)+C(J,K,I)*BM(I)
      DO 400 J=1,2
      CALL       BM2(MM,BM,J,A01,VV,EL,U,Y,DELX,XB,H,P)
      SUM=0 ; DO 395 I=1,NM1
  395 SUM=C(J,N,I)*BM(I)+SUM
      BM(N)=(YD(J,N)-SUM)/C(J,N,N)
      DO 400 K=1,N ; YD(J,K)=0 ; DO 400 I=1,N
  400 YD(J,K)=YD(J,K)+C(J,K,I)*BM(I)
C
  401 WAS=0
      RETURN ; END
$DATA
```

APPENDIX C

COMPUTER PROGRAM VARIABLES

Table 1. Computer Program Variables

Variable	Description
ARO(J)	Area parameter, A_o, of channel, J.
AR1(J)	Area parameter, A, of channel, J.
BM(K)	The right handside of the matrix.
C(I,J,K)	The coefficient matrix for the Channel I, J and K represent the location in the square matrix.
DA	Shape function, N_1.
DB	Shape function, N_2.
DELX	Distance step, ΔX.
DELT	Time step, Δt.
EL(J)	Element length of the channel, J.
FP	Corresponds to the distance, D, in the shape function when multiplied by the element length, ℓ.
G	Acceleration due to gravity.
N	Number of nodal points in each channel.
NA	Iteration count while using the Predictor-Corrector.
NC	Number of channels in the system.
P(I)	The highest power of the polynomial that represents the shape function for the channel, I.
PRØ(J)	Wetted perimeter parameter, P_o, of channel, J.
PR1(J)	Wetted perimeter parameter, P_1, of channel, j.
QD(J,K)	Time derivative of U at the element J and node K.
QD11(I,J)	Time derivative of U of the channel 1 at node 1.

QD21(I,J)	Time derivative of U of the channel 2 at node 1.
SF1, SF2	Energy slopes at the beginning and end of an element.
U(J,I)	Velocity of the channel J, node I.
YF and UF	The values of η and U respectively at an instant to be used in the Euler Predictor-Corrector.
Y(J,I)	Instantaneous water level of the channel J, node I.
YD(J,K) YD(J,K)	Time derivative of η at the channel J and node K.
YD33(I,J)	Time derivative of η of the channel 3 at node 2.

APPENDIX D

COMPUTED TIDAL FLUCTUATIONS IN CAROLINA BEACH INLET CHANNELS.

TABLE 2. COMPUTED TIDAL FLUCTUATIONS IN CAROLINA BEACH INLET CHANNELS.

TIME (HRS.)	AIWW (SOUTH) DM 156 (STATION/RANGE 1)					
	FLOW COND.	TIDE NODE 1		FLOW COND.	TIDE NODE 2	
		(Ft.)	(M)		(Ft.)	(M)
0800	EBB	2.97	0.904	EBB	2.772	0.845
0830		2.45	0.745		2.293	0.699
0900		2.24	0.681		2.021	0.616
0930		1.987	0.605		1.696	0.517
1000		1.311	0.399		1.142	0.348
1030		0.996	0.303		0.823	0.251
1100		0.524	0.160		0.353	0.108
1130		0.071	0.022		0.073	0.022
1200		0.201	0.061		0.349	0.106
1230		0.723	0.220		0.726	0.221
1300		1.113	0.339		1.064	0.324
1330		1.156	0.352		1.235	0.376
1400		1.484	0.452		1.350	0.411
1430	EBB	1.560	0.475	EBB	1.264	0.385
1500	FLOOD	1.002	0.305	FLOOD	0.986	0.300
1530		0.644	0.196		0.674	0.205
1600		0.251	0.076		0.136	0.041
1630		0.314	0.096		0.429	0.131
1700		0.911	0.278		0.911	0.278
1730		1.803	0.550		1.616	0.493
1800		1.974	0.602		1.879	0.570
1830		2.318	0.707		2.230	0.680
1900		2.837	0.865		2.778	0.847
1930		2.545	0.776		2.625	0.770
2000		3.132	0.955		2.886	0.880
2030	FLOOD	2.361	0.720	FLOOD	2.268	0.691
2100						

TABLE 2. COMPUTED TIDAL FLUCTUATIONS IN CAROLINA BEACH INLET CHANNELS (CONT.).

TIME (HRS.)	AIWW (NORTH) DM 150 (STATION/RANGE 2)					
	FLOW COND.	TIDE NODE 1		FLOW COND.	TIDE NODE 2	
		(Ft.)	(M)		(Ft.)	(M)
0800	EBB	2.940	0.896	EBB	2.776	0.846
0830	↑	2.434	0.742	↑	2.313	0.705
0900		2.221	0.677		2.049	0.624
0930		1.977	0.602		1.754	0.534
1000		1.324	0.403		1.209	0.368
1030		1.025	0.312		0.907	0.276
1100		0.576	0.176		0.455	0.139
1130		0.077	0.024		0.028	0.009
1200		0.234	0.071		0.277	0.084
1230		0.595	0.181		0.674	0.205
1300		0.992	0.302		0.992	0.302
1330	↓	1.356	0.413	↓	1.196	0.364
1400	EBB	1.442	0.439	EBB	1.363	0.415
1430	FLOOD	1.222	0.372	FLOOD	1.261	0.384
1500	↑	1.153	0.351	↑	0.989	0.301
1530		0.890	0.271		0.657	0.200
1600		0.067	0.020		0.099	0.030
1630		0.527	0.161		0.438	0.134
1700		0.901	0.275		0.424	0.282
1730		1.705	0.520		1.652	0.504
1800		1.941	0.592		1.902	0.580
1830		2.335	0.712		2.269	0.692
1900		2.850	0.869		2.794	0.852
1930		2.571	0.784		2.532	0.772
2000	↓	3.106	0.947	↓	2.889	0.881
2030	FLOOD	2.331	0.711	FLOOD	2.272	0.693

TABLE 2. COMPUTED TIDAL FLUCTUATIONS IN CAROLINA BEACH INLET CHANNELS (CONT.).

TIME (HRS.)	INLET GORGE (STATION/RANGE 3)					
	FLOW COND.	TIDE NODE 1		FLOW COND.	TIDE NODE 2	
		(Ft.)	(M)		(Ft.)	(M)
0800	EBB	2.766	0.843	EBB	2.454	0.748
0830	↑	2.264	0.690	↑	2.188	0.667
0900		1.983	0.604		1.822	0.555
0930		1.622	0.494		1.393	0.424
1000		1.055	0.321		0.943	0.287
1030		0.730	0.223		0.490	0.149
1100		0.255	0.078		0.110	0.034
1130		0.149	0.045		0.211	0.064
1200		0.425	0.129		0.510	0.155
1230		0.789	0.240		0.779	0.237
1300	↓	1.077	0.328		0.995	0.303
1330		1.245	0.379	↓	1.166	0.355
1400	EBB	1.369	0.417	EBB	1.205	0.367
1430	FLOOD	1.264	0.385	FLOOD	1.113	0.339
1500	↑	0.986	0.300	↑	0.877	0.267
1530		0.671	0.204		0.513	0.156
1600		0.139	0.042		0.083	0.025
1630		0.399	0.122		0.399	0.122
1700		0.862	0.263		0.934	0.285
1730		1.564	0.477		1.419	0.433
1800		1.833	0.559		1.816	0.554
1830		2.178	0.664		2.141	0.653
1900		2.755	0.840		2.410	0.735
1930		2.512	0.766		2.594	0.791
2000	↓	2.879	0.878	↓	2.532	0.772
2030	FLOOD	2.266	0.691	FLOOD	2.174	0.663

APPENDIX E

COMPUTED TIDAL VELOCITIES IN CAROLINA BEACH INLET CHANNELS.

TABLE 3. COMPUTED TIDAL VELOCITIES IN CAROLINA BEACH INLET CHANNELS.

TIME (HRS.)	AIWW (SOUTH) DM 156			(STATION/RANGE 1)		
	FLOW COND.	VELOCITY NODE 2		FLOW COND.	VELOCITY NODE 2	
		v (Ft./Sec.)	v (M/Sec.)		v (Ft./Sec.)	v (M/Sec.)
0800	EBB	0.768	0.234	EBB	0.810	0.247
0830	↑	1.483	0.452	↑	1.860	0.567
0900		2.159	0.658		2.185	0.666
0930		2.753	0.839		3.120	0.951
1000		3.228	0.984		3.484	1.062
1030		3.560	1.085		3.783	1.153
1100		3.727	1.136		4.163	1.269
1130		3.724	1.135		4.026	1.227
1200		3.543	1.080		3.766	1.148
1230		3.202	0.976		3.461	1.055
1300		2.720	0.829		3.041	0.927
1330		2.119	0.646		2.323	0.708
1400		1.440	0.439		1.207	0.368
1430	↓	0.722	0.220	↓	0.584	0.178
1500	EBB	0.003	0.001	EBB	0.095	0.029
1530	FLOOD	0.673	-0.205	FLOOD	1.152	-0.351
1600	↑	1.263	-0.385	↑	1.926	-0.587
1630		1.742	-0.531		1.880	-0.573
1700		2.073	-0.632		2.323	-0.708
1730		2.241	-0.683		2.592	-0.790
1800		2.234	-0.681		2.274	-0.693
1830		2.057	-0.627		2.575	-0.785
1900		1.716	-0.523		1.686	-0.514
1930		1.234	-0.376		1.230	-0.375
2000	↓	0.633	-0.193	↓	0.728	-0.222
2030	FLOOD	0.046	0.014	FLOOD	0.663	0.202
2100						

TABLE 3. COMPUTED TIDAL VELOCITIES IN CAROLINA BEACH INLET CHANNELS (CONT.)

TIME (HRS.)	AIWW (NORTH) DM 150 (STATION/RANGE 2)					
	FLOW COND.	VELOCITY NODE 1		FLOW COND.	VELOCITY NODE 2	
		V (Ft./Sec.)	V (M/Sec.)		V (Ft./Sec.)	V (M/Sec.)
0800	EBB	0.614	0.187	EBB	0.650	0.198
0830		1.188	0.362		1.499	0.457
0900		1.729	0.527		1.736	0.529
0930		2.201	0.671		2.484	0.757
1000		2.582	0.787		2.789	0.850
1030		2.848	0.868		3.031	0.924
1100		2.982	0.909		3.287	1.002
1130		2.979	0.908		3.127	0.953
1200		2.835	0.864		3.071	0.936
1230		2.562	0.781		2.943	0.897
1300		2.175	0.663		2.182	0.665
1330		1.696	0.517		1.709	0.521
1400		1.152	0.351		1.526	0.465
1430	EBB	0.577	0.176	EBB	0.325	0.099
1500	FLOOD	0.003	0.001	FLOOD	0.499	-0.152
1530		0.538	-0.164		0.558	-0.170
1600		1.010	-0.308		1.168	-0.356
1630		1.391	-0.424		1.726	-0.526
1700		1.657	-0.505		2.129	-0.649
1730		1.791	-0.546		2.096	-0.639
1800		1.788	-0.545		1.739	-0.530
1830		1.647	-0.502		2.021	-0.616
1900		1.375	-0.419		1.322	-0.403
1930		0.988	-0.301		0.997	-0.304
2000		0.509	-0.155		0.610	-0.186
2030	FLOOD	0.036	0.011	FLOOD	0.531	0.162

TABLE 3. COMPUTED TIDAL VELOCITIES IN CAROLINA BEACH INLET CHANNELS (CONT.)

TIME (HRS.)	INLET GORGE (STATION/RANGE 3)					
	FLOW COND.	VELOCITY NODE 1		FLOW COND.	VELOCITY NODE 2	
		V (Ft./Sec.)	V (M/Sec.)		V (Ft./Sec.)	V (M/Sec.)
0800	EBB	1.014	0.309	EBB	1.033	0.315
0830	↑	2.310	0.704	↑	2.385	0.727
0900		2.677	0.816		2.759	0.841
0930		3.829	1.161		4.134	1.260
1000		4.203	1.281		4.488	1.368
1030		4.524	1.379		4.780	1.457
1100		4.875	1.486		5.095	1.553
1130		4.596	1.401		4.731	1.442
1200		4.344	1.324		4.501	1.372
1230		3.996	1.218		4.131	1.259
1300		3.192	0.973		3.235	0.986
1330		2.438	0.743		2.470	0.753
1400	↓	1.654	0.504	↓	1.647	0.502
1430	EBB	0.545	0.166	EBB	0.433	-0.132
1500	FLOOD	0.256	-0.078	FLOOD	0.404	-0.123
1530	↑	1.056	-0.322	↑	1.204	-0.367
1600		1.962	-0.598		2.162	-0.659
1630		2.343	-0.714		2.530	-0.771
1700		2.946	-0.898		3.156	-0.962
1730		3.173	-0.967		3.425	-1.044
1800		2.729	-0.832		2.736	-0.834
1830		3.159	-0.963		3.192	-0.973
1900		2.090	-0.637		2.165	-0.660
1930		1.539	-0.469		1.637	-0.499
2000	↓	0.932	-0.284	↓	0.971	-0.296
2030	FLOOD	0.820	0.250	FLOOD	1.115	0.340